QUANTIFYING THE ABILITY OF RF-AMIDE NEUROPEPTIDE ANALOGS TO PROMOTE AMYLOIDOSIS OF RECOMBINANT HUMAN PRION PROTEIN

by

Shobha Gokul, M.Sc.

A thesis submitted to the Graduate Council of
Texas State University in partial fulfillment
of the requirements for the degree of
Master of Science
with a Major in Biochemistry
December 2015

Committee Members:

Steve Whitten, Chair

Kevin Lewis

Karen Lewis

FAIR USE AND AUTHOR'S PERMISSION STATEMENT

Fair Use

Duplication Permission

DEDICATION

TO MY HUSBAND GOKUL SRINIVASAN

ACKNOWLEDGEMENTS

I would like to thank my research advisor, Dr. Steve Whitten for his continued support and patient guidance in the completion of this work. My sincere gratitude for his kind encouragement and valuable inputs. I gratefully acknowledge my committee members Dr. Kevin Lewis and Dr. Karen Lewis for their critical review of my research project. I would like to express my gratitude to PREM-NSF for funding this project which allowed me to undertake this research. I am thankful to my lab colleague Paul Ford who helped me in many ways. I would also like to thank my other lab colleagues Leona Martin, Lance English and Erin Tilton for their assistance. Special thanks to my husband Gokul Srinivasan for his persistent confidence in me and for encouraging me to pursue my dreams.

TABLE OF CONTENTS

Page

LIST OF FIGURES

Figure **Page**

1. INTRODUCTION

Central to many life processes is the requirement for regulating biological activity. At the molecular level, this is often accomplished by interactions between various biomolecules and concomitant conformational changes in structure that are coupled to these interactions. Owing to the tight coupling of structure and function, changes in biomolecular structure often result in activity changes. Here, we have investigated the ability of short synthetic peptides to promote large-scale structure conversions in natively-folded and stable recombinant prion protein to 1) study mechanisms for regulating the biological activities of proteins via binding interactions and 2) test for possible roles of naturally occurring neuropeptides in the prion misfolding disorders.

1.1 Ligand Effects on Protein Structure

Proteins are essential biomolecules that perform a vast array of cellular functions in support of life processes. Every protein has a precise order of amino acids in its polypeptide chain that defines its primary structure. The molecular interactions between amino acids in a polypeptide chain and between the chain and solvent allow the protein to fold to a specific three dimensional (3-D) structure that specifies its function. The correctly folded 3-D structure of a protein is known as its native state. Studies show, however, that the native state of a protein is more accurately viewed as an ensemble of closely related, transiently populated, and interconverting conformational states.[1] The conformational fluctuations experienced by proteins can be modulated by interactions

with other molecules referred to as ligands, enabling a protein to switch between different functional states.[2] The ability of a protein to recognize, bind, and respond to a ligand is critical for regulating biological activity. Investigations of protein-ligand interactions therefore could provide key molecular details for understanding the structure-function relationships and regulatory properties of proteins.

Prior work has developed an ensemble-based description of protein structure[3] that has been successful at modeling ligand-induced effects on the conformational fluctuations of proteins and its role in regulating biological activity.[1,4-5] Those studies indicated that not all possible binding sites for a ligand in a protein have the capability of modulating protein structure for regulatory purposes.[4-5] True regulatory binding sites seemed to exhibit increased abilities for propagating binding energy to distant positions in the protein, relative to what was observed for decoy binding sites,[5] and causing coordinated changes in structure.[4] To test these observations, the present study was initiated to determine if regulatory binding sites could be predicted using these ensemble-based models of protein structure. For this, we chose the human Prion Protein (hPrP) as our test system since the structure of native hPrP[6] is publically available from the Protein Data Bank (PDB), allowing for computer simulations of the hPrP conformational ensemble and the prediction of possible binding sites. Moreover, the activity of hPrP in biological systems is coupled to a dramatic structural change, one that converts its monomeric native state that is rich in alpha helices to insoluble oligomers that are rich in beta structure and show amyloid fibril character.[7] Accordingly, ligand-induced conversions between these two structural states should be straightforward to detect since the structure changes are not subtle. An additional benefit to this system is that ligand

cofactors are known to contribute to the structural conversion of native hPrP to amyloid[8] but the cofactor identities and binding site locations have not yet been established.[9]

In work that was presented previously in the Master of Science (MS) theses of Melody Adam[10], Ryan Maldonado[11], James Campbell[12], and Reagan Meredith (unpublished), a regulatory site on the C-terminal helix of native hPrP was predicted to be present based upon computer simulations of the hPrP conformational ensemble and the response of the hPrP ensemble to ligand perturbations. These results are summarized in Figure 1.1 and show that the central region of the C-terminal helix has an enhanced ability for propagating binding energy relative to other regions of the native hPrP structure. The C-terminal helix contains tyrosine residues at positions 218, 225, and 226 and glutamate residues at positions 211 and 219. To exploit this pattern of phenol rings and negative charge on the helix surface, short polypeptides with complementary patterns of positive charge and phenol rings from the sequence lysine-phenylalanine-alanine-lysine-phenylalanine (KFAKF) were designed as first generation ligands. Melody Adam and Reagan Meredith showed that polypeptides containing the KFAKF motif were able to convert native hPrP to beta-rich insoluble oligomers. Short 5-residue linear peptides containing just the KFAKF sequence did not convert native hPrP to amyloid-like particles, but a cyclic peptide, cyclo-CGGKFAKFGGC, did interact with native hPrP to promote fibril conversion.[10] Based upon these results, Ryan Maldonado tested if synthetic homologs to mammalian neuropeptides called RF-amide neuropeptides could promote amyloid conversion of native hPrP, owing to the similarities between the KFAKF motif and the RFMRF sequence that is common to this class of natural and biologically active peptides.[11] RF-amide neuropeptides have arginine and amidated phenylalanine residues at

the C-terminal end.[13] They are highly conserved from invertebrates to mammalian species and have been shown to have neuroendocrine and neuro-modulatory functions.[13] The main objective of the current work is to establish the concentration dependence of these RF-amide peptides for converting native hPrP to amyloid-like fibrils.

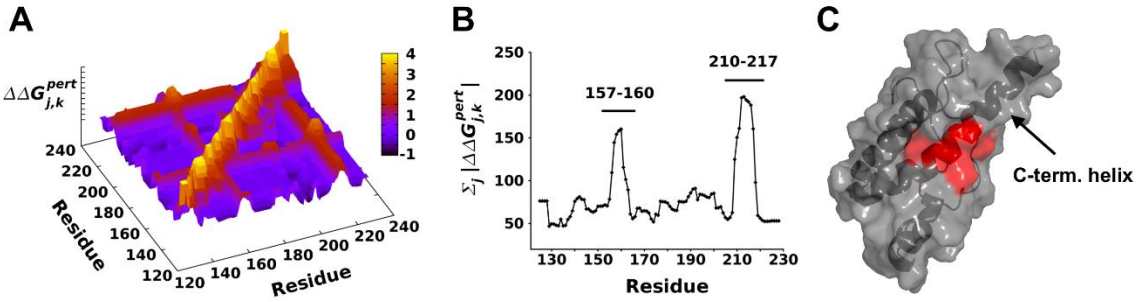

Figure 1.1 Location of sites that propagate binding energy efficiently in the native hPrP structure. In other proteins, known regulatory sites correlated with positions that were efficient at propagating binding energy in native structures relative to decoy sites.[5] **A)** In the computer simulations, an energetic perturbation applied at site *j* and the effect on native stability at site *k* ($\Delta\Delta G_{j,k}^{pert}$) was calculated. Large $\Delta\Delta G$ values along the diagonal represent $j = k$ calculations. These data show that energetic perturbations at some sites propagated to distant residue positions better than what was calculated for other sites, causing a subset of sites *j* with relatively large $\Delta\Delta G$ values at sites $k \neq j$. **B)** To represent this general observation, the magnitude of $\Delta\Delta G$ values owing to each residue position *j* were summed to show that residues 157-160 and 210-217 were most efficient at propagating energetic perturbations and are possible regulatory sites. **C)** Residues 210-217 reside at the center of the C-terminal helix whereas residues 157-160 pack directly against the buried underside of the central region of this helix.

1.2 Amyloid and the Protein Misfolding Disorders (PMDs)

To attain properly folded 3-D architecture, proteins follow specific folding pathways which drive them towards a thermodynamically stable final structure.[14] Protein folding occurs primarily in specialized compartments of the Endoplasmic Reticulum (ER).[15] The reducing environment in the ER can sometimes lead to protein folding problems, which are combatted by chaperones.[15] Alternate folding pathways can cause protein misfolding leading to alteration or loss of biological function.[14] To avoid this problem, chaperones assist misfolded proteins to restore their correct conformation.[15] However, if the misfolded proteins are unable to attain their correct structure, they are immediately recognized and targeted for degradation in the system. In the case of Protein Misfolding Disorders (PMDs), misfolded structures tend to aggregate in cells forming degradation-resistant plaques.[14] Plaques that resist normal cellular degradation are typically composed of insoluble and fibrous structures called amyloid fibrils. The accumulation of plaques in cells can trigger a cascade of events leading to progressively degenerative diseases and ultimately death.[14] Some examples of PMDs include Transmissible Spongiform Encephalopathies (TSEs), Parkinson's disease, and Alzheimer's disease.[14]

1.3 Prion Protein

The human Prion Protein (hPrP) is a membrane-associated protein most abundantly expressed in brain cells.[16] It is anchored to the cell membrane with glycosylphosphatidylinositol moiety at its C-terminal end.[16] The hPrP gene is located on the short arm of chromosome 20.[17] The length of the primary sequence of hPrP is 230

amino acids. During post-translational modification, the N-terminal signal peptide involved in protein trafficking is removed to form the mature hPrP with 208 amino acids.[6] The N-terminal region of mature hPrP has a flexible disordered "tail", whereas the C-terminal region contains a stable globular domain with three-α helices and two β-strands.[6, 18] See Figure 1.2 for a cartoon representation of the native structure of the stable regions of hPrP. PrP^{C} and PrP^{Sc} are two conformational isoforms of prion protein. PrP^{C} is the natively folded cellular protein that is rich in alpha helix.[18] PrP^{Sc} is the misfolded amyloid form that is rich in beta-sheet content.[18] Although the exact biological role of PrP^{C} is not yet clear, some of the postulated roles include cellular trafficking of copper ions, signal transduction, neuronal cell adhesion, neurotransmitter metabolism, regulation of apoptosis, and oxidative stress relief.[19]

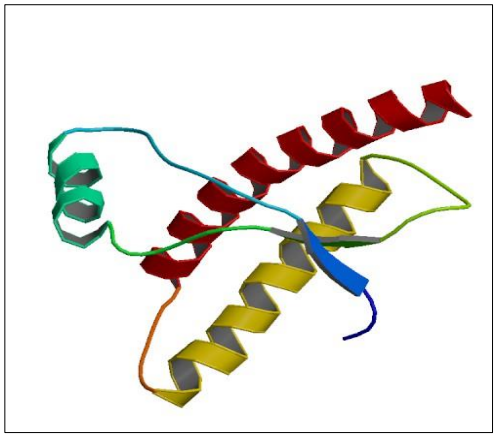

Figure 1.2 Solution NMR structure of natively folded recombinant hPrP(125-230).[6] Cartoon structure of hPrP was colored from N-terminal to C-terminal with a rainbow color gradient from violet to red respectively. PDB accession code: 1QLX.

1.4 Prion Misfolding Disorders

Prion disorders, also known as TSEs, are a group of neurodegenerative diseases caused from the accumulation of misfolded prion proteins as amyloid fibers in neurons.[14] Some of the diseases under the TSE class include the human disorders Kuru, Familial Fatal Insomnia (FFI), Gerstmann-Straussler-Scheinker syndrome, and Creutzfeldt-Jacob disease (CJD). Also, there is Bovine Spongiform Encephalopathy (BSE) in cows; Scrapie in sheep and goats; and Chronic Wasting Disease in elk, deer, and moose.[20] In 1982, Stanley Prusiner proposed the "Protein Only Hypothesis" for transmission of TSEs.[8] According to this hypothesis, misfolded prions, PrP^{Sc}, interact with cellular prion protein to convert PrP^{C} into new PrP^{Sc} particles and thus propagate the disease.[8] Since then, several studies have been conducted to test this hypothesis.[20] Some of these studies suggest that additional cofactors or ligands are needed to self-propagate PrP^{Sc} material.[20] The molecular mechanism of PrP^{C} conversion to PrP^{Sc}, however, still remains unclear.

1.5 Amyloid Fibril Structure

Amyloid fibrils are highly ordered structures formed from self-assembly of misfolded proteins.[21] They were termed as "amyloids" by Rudolf Virchow in 1984 due to their ability to produce positive iodine staining reaction, a characteristic of starchy materials.[22] Under an electron microscope they appear as non-branched, long filaments with diameter of 6-12 nm.[21] Figure 1.3 shows a Scanning Electron Microscope (SEM) image of recombinant hPrP converted to amyloid fibers using cyclo-CGGKFAKFGGC. In general, amyloid fibers are insoluble in water and non-crystalline.[22] These fibers can have lengths of up to a micrometer and molar masses in the megadalton range.[23] X-ray

diffraction studies confirm that amyloid fibers are rich in beta-sheets and have a characteristic structural fold referred to as cross-beta motif.[21] Several studies indicate that oligomeric pre-fibrillar structures are responsible for the toxicity of amyloid-based diseases.[23]

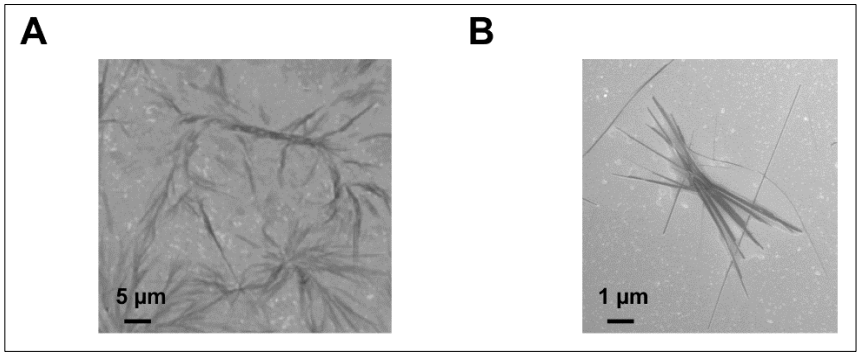

Figure 1.3 Fibril structure of recombinant hPrP misfolded by the peptide cyclo-CGGKFAKFGGC. These Scanning Electron Microscopy (SEM) images were obtained by Reagan Meredith (unpublished work) and Dr. Carlos Gonzalez Garrido using standard SEM techniques. The fibrils in panel **A** were untreated whereas panel **B** shows fibrils that were digested with proteinase K.

1.6 Project Goals

The goal of this thesis project was to quantify the ability of synthetic analogs of the RF-amide neuropeptides to induce amyloid conversion of natively folded recombinant hPrP. The demonstration that endogenous peptides with sequences similar to the KFAKF motif could promote amyloid misfolding of native hPrP would provide evidence that native regulatory sites can be predicted from protein structures using ensemble methods. Since the synthetic peptides are analogs of RF-amide neuropeptides

that naturally express in mammalian brain, the results also would report on the potential for the RF-amide class of neuropeptides to contribute to prion disorders. To accomplish these goals, the experimental strategies listed below were followed:

a) Express recombinant hPrP in bacterial cells and then isolate hPrP from bacterial lysates using standard recombinant DNA techniques, cell lysis protocols, and anion exchange and affinity chromatography.

b) Determine the level of purity of recombinant hPrP that was isolated from bacterial lysates using Sodium Dodecyl Sulfate Polyacrylamide Gel Electrophoresis (SDS-PAGE) and silver staining.

c) Establish that recombinant hPrP was correctly folded to its native structure using circular dichroism (CD) spectroscopy to verify native alpha helical structural and monitor heat-induced unfolding of native hPrP to show that the native state is stable under the experimental conditions of the amyloid conversion reactions.

d) Individually mix synthetic analogs of the RF-amide neuropeptides FMRF-amide, KGGFSFRF-amide, FLFQPQRF-amide and VPNLPQRF-amide with recombinant native hPrP at the peptide concentrations 1.0 mM, 0.1 mM and 1.0 μM to determine the concentration-dependence in the ability of these RF-amide analogs to cause amyloid misfolding of native hPrP. The reaction mixtures were performed under physiological-like conditions for different lengths of time (0-72 hours) to determine the time required

for amyloid particles to form under the different peptide concentrations and for the different peptide sequences.

e) Detect amyloid conversion of native hPrP using Semi-Denaturing Detergent-Agarose Gel Electrophoresis (SDD-AGE) and a Proteinase K (PK) digestion assay. SDD-AGE detects amyloid fibrils by their resistance to detergent dissolution, whereas non-amyloid aggregates are solubilized by 2% SDS.[24] Thus, SDD-AGE can differentiate between amyloid fibrils and other types of oligomers and aggregates that may form during the course of a misfolding reaction. PK digestion assays detect amyloid fibrils by their partial resistance to proteolysis. Native hPrP is readily digested by PK, however, amyloid fibrils form PK resistant fragments with sizes that range from 4-16 kDa. These resistant fragments are the beta-sheet rich core of amyloid fibrils.[25] Therefore, samples with amyloid fibers show protease resistant bands on SDS-PAGE that can be visualized using silver staining techniques.

2. MATERIALS AND METHODS

2.1 Materials

All chemicals and reagents used for this project were Molecular grade or higher. Synthetic peptides were synthesized commercially to 98% purity by GenScript (Piscataway, NJ) and Peptide 2.0 (Chantilly, VA). Water used in sample preparation was filtered and deionized by a Millipore Milli-Q purification unit (Billerica, MA). Glassware, pipette tips and other basic equipment were sterilized with a HICLAVE HV-50 autoclave vessel by Hirayama (Westbury, NY).

2.2 Expression and Purification of Recombinant Prion Protein

2.2.1 Cloning and Transformation

Recombinant hPrP was expressed in *Escherichia coli* (*E. coli*) cells using the pJexpress bacterial plasmid (pJexpress 404). This plasmid contained an ampicillin resistance gene and a bacteriophage T5 promoter sequence upstream of the insertion site for Isopropyl β-D-1-thiogalactopyranoside (IPTG) induced expression. The hPrP amino acid sequence for residues 23-230 was inserted into the pJexpress plasmid. The amino acid sequence used in our study was taken from a wild-type consensus of hPrP as shown in Figure 2.1. Residues 1-22 constitute signal peptide for sorting and trafficking of hPrP, and residues 231-246 are removed during protein maturation. Therefore, the signal peptide and maturation sequences were not included for bacterial expression. Plasmids

with hPrP inserts were solubilized in DNA grade sterile water at a concentration of 1 ng/μL in sterile cryovial tubes and stored at -80°C.

1 MANLGCWMLV LFVATWSDLG LCKKRPKPGG WNTGGSRYPG
QGSPGGNRYP PQGGGGWGQP
61 HGGGWGQPHG GGQGQPHGGG WGQPHGGGWG QGGGTHSQWN
KPSKPKTNMK HMAGAAAAGA
121 VVGGLGGYVL GSAMSRPIIH FGSDYEDRYY RENMHRYPNQ
VYYRPMDEYS NQNNFVHDCV
181 NITIKQHTVT TTTKGENFTE TDVKMMERVV EQMCITQYER ESQAYYKRGS
SMVLFSSPPY
241 ILLISFLIFL IVG

Figure 2.1 Amino acid sequence of full length hPrP. Residues 1-22 constitute the signal peptide for protein trafficking, and residues 231-246 are removed during protein maturation. In the study presented here, we have used the residues 23-230 for bacterial expression.

Transformation of BL21 (DE3) pLysS competent cells by Novagen (Darmstadt, Germany) were done by adding 5-10 μL of plasmid in 50 μL of the competent cells suspended in 60 mM calcium chloride. The mixture was placed on ice for 5 minutes, heat shocked in a water bath at 42°C for 30 seconds, and then placed on ice again for 2 minutes. The mixture was allowed to cool to room temperature and 250 μL of Super Optimal Broth (SOC) was added. 150 μL of the cells were spread on Lysogeny Broth (LB) agar plates containing 100 μg/mL of ampicillin. These plates were incubated

overnight at 37°C. An Erlenmeyer flask containing 20 mL of LB and 100 μg/mL of ampicillin was aseptically inoculated with a single colony of *E. coli* cells transformed with pJexpress plasmid containing hPrP gene. The 20 mL cell culture was incubated overnight in a rotary incubator (Max*Q, MIDSCI, St. Louis, MO) at 30°C with 170 RPM orbital rotation. Glycerol stocks of the transformed cell cultures were made by adding 800 μL of cell culture to 200 μL of sterile 80% glycerol, and stored in sterile cryovial tubes at -80°C.

2.2.2 Expression of Recombinant hPrP

Aseptic dab of *E. coli* cells from glycerol stocks were spread onto an LB agar plate containing 100 μg/mL of ampicillin. The plate was incubated at 37°C overnight. A single colony from the plate was inoculated in 20 mL of LB broth with 100 μg/mL of ampicillin. The culture was grown at 30°C for 16 hours on an orbital shaker (Max*Q, MIDSCI, St. Louis, MO) with 170 rpm agitation. 4 mL of the incubated culture was transferred to each of 4 flasks containing 196 mL LB broth with ampicillin. The flasks were incubated for 2.5 hours at 37°C. Once an OD_{600} of 0.6 was achieved, IPTG was added to a final concentration of 1.0 mM to induce hPrP expression. IPTG induction was done for 4.5-5 hours. Induced cells were centrifuged at 8,000 RPM at 4°C for 20 minutes using a Beckman J2-21 centrifuge with a JA-14 rotor (Beckman-Coulter, Brea, CA). The supernatant was discarded and cell pellets were stored at -20°C.

2.2.3 Purification of Recombinant hPrP

Frozen cell pellets were lysed in 20 mL lysis buffer (10 mM Tris-HCl, 2 mM EDTA, 100 mM NaCl, 100 μg/mL lysozyme, pH 7.5). The suspension was incubated for 30 minutes at 37°C to allow lysozyme to degrade the bacterial cell wall. Sonication was performed with the cell suspension in thermal contact with packed ice, to mitigate heating of the sample, and using a Bronson Sonifier S-450A (Danbury, CT) set to an output control of 5, duty cycle of 80% with three, one minute pulses separated by one minute rest periods. Following sonication, 1 ml of 10% Triton X-100 was added to the cell lysate to a final concentration of 0.5% and the sample was centrifuged at 22,000 x g, 4°C for 1.5 hrs. The supernatant was discarded following centrifugation. The cell pellet was resuspended in 10 mL of resuspension buffer (8 M urea, 20 mM Tris-HCl, 100 mM NaCl, pH 8.0) and incubated at overnight at 4°C.

The next day, the solution was prepared for column chromatography by centrifuging at 10,000 x g, 4°C for 20 minutes. The supernatant was loaded onto a DE52 anion exchange column (GE healthcare, New Orleans, LA). DE52 media was used to remove any contaminating proteins, nucleic acids, and proteases from the sample. Protein purification was conducted on a Biologic LP system from Bio-Rad Laboratories (Hercules, CA), protein elution was monitored by UV absorbance at 280 nM. The column media was prepared by adding the DE52 beads to a solution containing 20 mM Tris-HCl, 100 mM NaCl, pH of 3.5 and gently mixed on a stir plate for 10 minutes to allow the media to swell. Next the media was degassed by vacuum for 20 minutes. The media was then poured into a glass column and equilibrated with 20 mL of equilibration buffer (8 M urea, 20 mM Tris-HCl, 100 mM NaCl, pH 8.0). The cell lysate was then passed through

the column followed by wash with equilibration buffer. The flow through and wash, which contained recombinant hPrP, was collected and saved for affinity chromatography.

The flow through sample was loaded onto an nickel(II)-nitriloacetate (Ni-NTA) agarose column to perform Immobilized Metal Affinity Chromatography (IMAC). The hPrP has a natural affinity for Ni-NTA and does not require the addition of a 6x-histidine tag for affinity purification. The media was regenerated prior to each re-use using SIGMA's manufacturing protocol. Following regeneration, the column media was equilibrated using 20 mL of equilibration buffer (8 M urea, 20 mM Tris-HCl, 100 mM NaCl, pH 8.0). The DE52 flow through was carefully loaded onto the column and then washed with equilibration buffer until UV absorbance signal returned to baseline. The column was then washed with 20 mL of Buffer A (20 mM Tris-HCl, 100 mM NaCl, pH 8.0) to remove urea. This was followed by wash with 20 mL Buffer B (20 mM Na_2HPO_4, 100 mM NaCl, pH 8.0) to aid protein refolding. Elution of recombinant hPrP was achieved by using imidazole as a competitive agent and by lowering the pH. The elution buffer used was 20 mM Na_2HPO_4, 100 mM NaCl, 500 mM imidazole, pH 4.5.

The purified sample was filtered with a 0.45 micron filter and subjected to dialysis. Dialysis was done using Spectra/Por dialysis tubing (Spectrum Laboratories, Ca). The purified protein was first dialyzed for 16 hours in 4 L of Dialysis Buffer 1 (10 mM Na_2HPO_4, pH 5.8), followed by 3 hours dialysis in 4 L of Buffer 2 (5 mM Tris-HCl, pH 8.5). The dialyzed protein sample was then filtered with a 0.45 micron filter to remove any pre-formed aggregates. Protein concentration was determined using an UV-Vis spectrophotometer (Bio-Rad, Hercules, CA) by measuring absorbance at 280 nm. Concentration of purified protein was then calculated using the Beer-Lambert law

($A=\varepsilon Cl$) with an extinction coefficient of 58780 $M^{-1}cm^{-1}$. SDS PAGE was used to assess the purity of the protein.

2.3 Purity Analysis Method

2.3.1 Sodium Dodecyl Sulfate Polyacrylamide Gel Electrophoresis (SDS-PAGE)

Purified samples were run on SDS-PAGE to confirm purification of hPrP. SDS is an anionic detergent that denatures the proteins in the sample and confers uniform negative charge to the linearized proteins. This allows separation of proteins according to their molecular weight based on their differential rate of migration through the gel. Purity of hPrP was confirmed by the presence of a single band around 23 kDa, which corresponds to the molecular weight of hPrP. Samples were mixed with Laemmli Sample Loading Buffer (62.5 mM Tris-HCl, 25 % glycerol, 2% SDS, 0.01 % bromophenol blue, 2-mercaptothanol, pH 6.8), boiled for 8 minutes and loaded onto the gel. Pre-cast polyacrylamide gels (4-20% acrylamide) from Bio-Rad (Hercules, CA) were used for this purpose. The gels were run at 200 V for 45 min in 1X TGS (25 mM Tris, 192 mM glycine, 0.1 % SDS, pH 8.3) running buffer.

2.3.2 Silver Nitrate staining of polyacrylamide gels

Following electrophoresis, proteins were detected by silver staining the polyacrylamide gels. Silver staining detects proteins at sensitivities as low as the nanogram range. The gel was initially soaked in fixer solution (125 mL methanol, 30 mL glacial acetic acid, 0.125 mL 37.5% formaldehyde, ddH_2O to 250 mL) for 30 minutes at room temperature and with gentle rocking. The gel was rinsed twice in 50% ethanol for

15 minutes for each wash. The gel was then sensitized by soaking for 1 minute in 5 mM sodium thiosulfate. The gel was rinsed 3 times with ddH_2O for 20 seconds each. The gel was then soaked in silver solution (12 mM silver nitrate and 0.02% formaldehyde) for 20 minutes at 4°C. Finally, the silver ions were reduced to metallic silver by treating the gel with 150 mL of a reducing buffer (300 mM sodium carbonate, 0.15 mM sodium thiosulfate, 0.02% formaldehyde) for 30 seconds to 2 minutes till an adequate degree of staining was achieved. The stained gel was then washed in ddH_2O to stop development and imaged.

2.4 Protein Structure Analysis by Circular Dichroism Spectroscopy

Circular dichroism (CD) spectroscopy is a technique used to determine secondary structure and folding properties of proteins.[26] It can distinguish between α helical, β sheet, and random coil conformations. The hPrP in its native state is predominantly rich in α helices. It consists of 3 large α helices that span residues 144-154, 173-194, and 200-228, and a small β sheet spanning residues 128-131 and 161-164. A CD spectrum of the purified protein sample was obtained using a Jasco J-710 spectropolarimeter (Easton, MD). N_2 gas was purged into the optical housing at a flow rate of 5 L/min. Sample was measured in a 1 mm quartz cuvette at a scan rate of 50 nm per minute in 5 nm steps and averaged over 12 scans per spectrum. The CD was blanked against 10 mM Na_2HPO_4, pH 6.0. The following equation was used to convert the raw output data from ellipticity to the normalized mean molar ellipticity (θ_{MRE}):

$$\theta_{MRE} = \theta \frac{M}{1 \times C \times l \times n} \left[\frac{deg \times cm^2}{dmol \times residue} \right]$$

where M is the molecular weight of hPrP (22.75 kDa), C is the molar protein concentration, *l* is the path length of the cuvette, and *n* is the number of residues in hPrP (207).

2.5 Peptide Induced Amyloid Conversion

Purified recombinant hPrP was mixed with synthetic RF-amide neuropeptides to prepare the amyloid conversion mixtures. The total reaction volume of each aliquot was 100 µL. It contained 4.3 µM hPrP and varying concentrations of the synthetic peptides in a 1 X Quic buffer (1X PBS, 0.4 % SDS, 0.4 % TritonX-100, pH 7.0). Reactions were run for different time points in a thermomixer (Eppendorf) at 37°C, 1500 RPM with 1 minute agitation and 1 minute rest cycles. Time trials per experiment were tested up to 72 hours. Reactions were stopped at different time points by freezing the samples at -20°C. Samples were frozen for up to a month prior to performance of the amyloid detection assays.

2.6 Amyloid Detection Methods

2.6.1 Semi-Denaturing Detergent Agarose Gel Electrophoresis

Semi-Denaturing Detergent Agarose Gel Electrophoresis (SDD-AGE) is an electrophoretic technique used for detection of amyloid fibers based on size and detergent insolubility. Amyloid fibers have a β-sheet rich core which makes them resistant to denaturation by 2% SDS. However, the monomeric prion protein and protein aggregates are susceptible to denaturation by the detergent.[24] Samples are run on agarose gel with 2% SDS. Agarose gels have larger pore sizes compared to polyacrylamide. This allows

smaller monomeric proteins to migrate faster through the pores, whereas movement of the larger oligomers gets restricted. Samples containing amyloid show a typical streaking pattern due to a range of oligomeric sizes. James Campbell optimized several parameters of the SDD-AGE protocol such as the gel thickness, electrophoretic conditions and capillary transfer method in his MS thesis.[12] The current work involves the use of Campbell's improved SDD-AGE protocol to detect amyloid conversion.

The SDD-AGE gel was prepared on a 10 cm x 15 cm casting tray with an 18 well comb. Agarose gel of concentration 1.8 % was prepared by heating 1.08 g of agarose in 60 mL of 1 X TAE (40 mM Tris-HCl, 20 mM acetic acid, 1 mM EDTA) for total of 3 minutes with gentle swirling every 30 seconds. Total volume of 60 mL generated thin gels with an approximate thickness of 0.4 cm, which according to Campbell's optimized protocol provides the best resolution of amyloids.[12] The agarose solution was then cooled for 8 minutes and 60 µL of 10 % SDS was added. The agarose solution was slowly poured onto the casting tray and care was taken to avoid air bubble formation. Any air bubbles formed were removed using a pipet tip prior to setting the comb. The casted gel was allowed to solidify by letting it cool for least 30 minutes at room temperature (RT). The gel was then placed in Bio-Rad Sub Cell GT (Hercules, CA) with pre-chilled 1X TAE buffer containing 0.1% SDS. Samples were mixed with SDD-AGE loading buffer (2 X TAE, 20 % glycerol, 8 % SDS, 1 % bromophenol blue) in a 4:1 ratio and incubated at room temperature for 7 minutes. Fifteen µL of this mixture was loaded into each well of the agarose gel. Electrophoresis was performed for 1.5 hours at 120 V.

Following electrophoresis, the gel was first rinsed in ddH_2O to remove any residual SDS, and then equilibrated in transfer buffer 1X Tris Buffered Saline (TBS) (20

mM Tris, 0.1 M NaCl, pH 7.5) for 15 minutes. A capillary transfer method was used to transfer the proteins on the gel to a nitrocellulose membrane. This method is simple, cost-effective, allows more number of samples to be processed and ensures efficient transfer of proteins from any sized gel without distortion. The capillary transfer stack was set up using a cleaned agarose gel rig as a transfer tray. Transfer trays were filled with the transfer buffer and four thin strips of blotting paper were used as wicks to allow transfer buffer to produce capillary action. A large piece of blotting paper was then soaked in TBS and placed on the wicks. The agarose gel was placed on the blotting paper with the wells facing down. The nitrocellulose membrane equilibrated in TBS was then placed on top of the gel and gently rolled with a roller to remove any air bubbles at the gel-membrane interface. Displacing any trapped air-bubbles is crucial to prevent any dead spots on the blot. Additional sheets of blotting paper and paper towels were placed on top of the membrane gel stack to assist with the capillary action. On top of the transfer stack, a 1kg weight was placed to promote contact between gel and the membrane. Capillary transfer was allowed to proceed for 12-16 hours. Following capillary transfer of proteins onto the membrane, western blot analysis was performed.

2.6.2 Western Blot Analysis

SDD-AGE results were analyzed using the western blot technique. The nitrocellulose membrane was removed from the transfer stack and washed in Tris-TWEEN buffer saline (T-TBS; 20 mM Tris, 0.1 M NaCl, 0.1 % TWEEN-20, pH 7.5) for five minutes. Next, the membrane was incubated for 1 hour with constant rocking in a blocking solution of 5 % dry milk in T-TBS. The membrane was then washed three times

for two minutes in T-TBS. This was followed by soaking the membrane for 1 hour in a solution containing dry milk, T-TBS and primary antibody on an orbital shaker. The primary antibody used was the 3F4 antibody (Covance, Princeton, NJ) at 1:10000 working concentration which binds to residues 109-112 of hPrP. After incubation, excess and unbound 3F4 was removed by washing the membrane three times with T-TBS for 10 minutes each. The membrane was then incubated in a secondary antibody for 1 hour. The secondary antibody consisted of anti-mouse IgG conjugated to horseradish peroxidase (GE Healthcare, Piscataway, NJ) diluted to 1:50,000 in T-TBS and dry milk. The membrane was then washed three times in T-TBS for 10 minutes each and allowed to dry. The ECL Prime chemiluminescence detection kit (GE Healthcare) was used to image detection. Chemiluminescence solution was applied to the membrane for 5 minutes while incubating in the dark. The membrane was then imaged using a ChemiDoc XRS+ imaging system (Bio-Rad, Hercules, CA). As shown in Figure 2.2, monomeric protein display a single band at 23 KDa, whereas, amyloid particles show smeared bands due to resistance to SDS denaturation. To test if random protein aggregates also show resistance to SDS denaturation, heat denaturation of hPrP was performed. As seen in Figure 2.3, no smeared bands was observed for heat denatured aggregates, indication random aggregates are not amyloids.

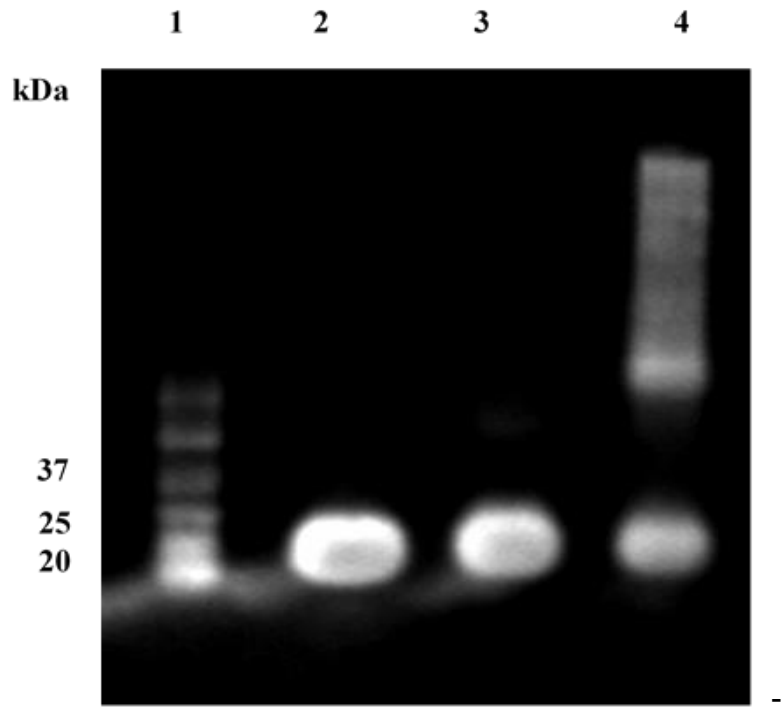

Figure 2.2 SDD-AGE detection of hPrP. SDD-AGE is used to detect the presence of amyloids. Western blot detection was done using the 3F4 antibody. Lane 1 shows a protein ladder with molecular weights labeled. Lanes 2-3 show the standard monomeric hPrP. Lane 4 shows amyloid particles displaying a typical streaking pattern on an SDD-AGE gel due to polydispersion of higher molecular weight oligomers.

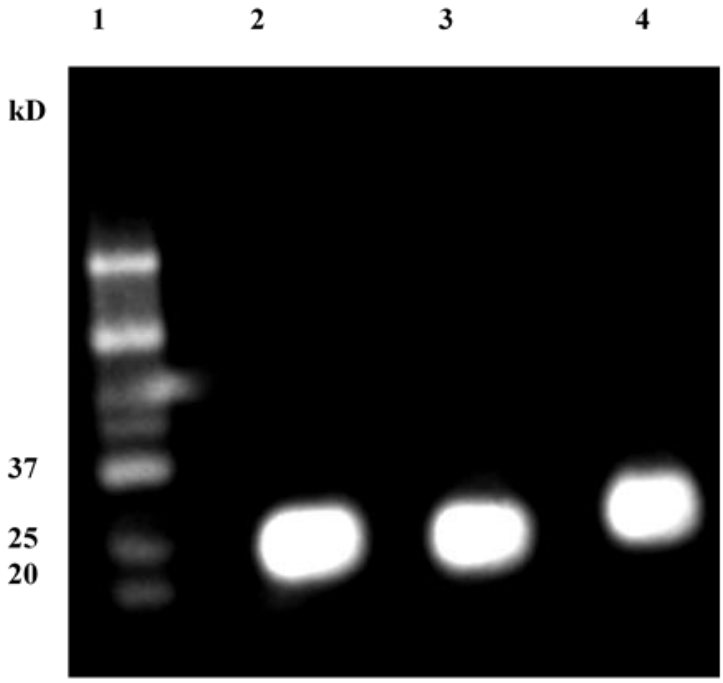

Figure 2.3 Heat denaturation of recombinant hPrP. The recombinant hPrP was subjected to heat denaturation by heating the sample above 90˚C for 10 minutes to form protein aggregates. Lane 1 shows a protein ladder with molecular weights labeled. Lane 2 shows untreated monomeric hPrP. Lanes 3-4 show heat-induced aggregates of hPrP. No streaking is observed in lanes 3-4 indicating protein denaturation does not produce SDS-resistant oligomers.

2.6.3 Proteinase K Digestion Assay

Proteinase K (PK) is a proteolytic enzyme that cleaves the bond adjacent to the carboxyl group of aliphatic and aromatic amino acids.[27] Native hPrP is readily digested by PK, however, amyloid fibrils have been shown to form PK resistant fragments with sizes that range from 4-16 kDa.[28] These resistant fragments are the beta-sheet rich core of amyloid fibrils[25] and can be easily observed on SDS-PAGE. Sample digestion was done by mixing 19 μL of sample (section 2.5) with 1 μL of 0.2 mg/mL PK and incubating in a thermomixer for 1 hour at 37°C with 600 RPM agitation. After PK digestion, the reaction was terminated by heating the samples with Laemmli sample loading buffer (2:3 ratio) at 95°C for 8 minutes to deactivate PK. The samples were then cooled for 10 minutes at RT, following which they were stored in freezer at -20°C until analysis by SDS-PAGE and silver staining (section 2.3.2). Figure 2.4 shows that monomeric protein get completely digested by PK, however, amyloid particles form PK resistant fragments.

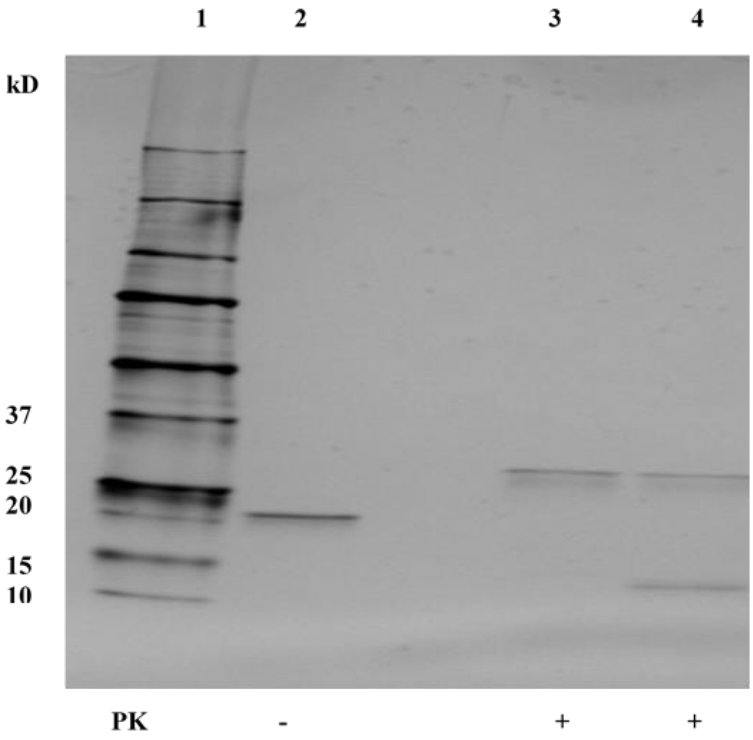

Figure 2.4 PK digestion assay. PK digestion assays are used to detect PK resistant fragments of amyloid particles. Lane 1 shows a standard protein ladder with molecular weights labeled to their corresponding bands. Lane 2 shows control undigested monomeric hPrP. Lane 3 contains monomeric hPrP digested using PK by the method described in section 2.6.3. Lane 4 contains amyloid particles as apparent by the band at ~14 kDa. Lanes 3-4 have bands at ~29 kDa corresponding to Proteinase K.

3. AMYLOIDOSIS OF RECOMBINANT HUMAN PRION PROTEIN INDUCED BY RF-AMIDE NEUROPEPTIDE ANALOGS

3.1 Introduction

Protein-peptide interactions are central to most biological processes in living cells. The function of a protein is closely associated with its structure and interaction with other molecules. Therefore, investigations of protein-peptide binding interactions could provide key molecular details to understand mechanisms for regulating the biological activities of proteins. The Whitten Group has developed a recombinant system to investigate these interactions using natively-folded and stable human Prion Protein (hPrP). In biological systems, the activity of hPrP is linked to a dramatic structural change involving conversion of its monomeric native state that is rich in alpha helices to insoluble amyloid oligomers that are rich in beta structure.[7] Conversions between the two structural states are not subtle and are straightforward to detect. Moreover, ligand cofactors are known to contribute to the structural conversion of native hPrP to amyloid[8], however, the cofactor identities and binding site locations have not yet been established.[9] Computer simulations predicted regulatory site on C terminal helix of hPrP. Initial investigations by the Whitten Group involved testing short synthetic peptides with a KFAKF motif targeting the predicted regulatory site in natively-folded recombinant hPrP to induce large-scale structural conversions to amyloids. The KFAKF motif was found to have sequence similarity to the RFMRF motif that is common to the class of natural and biologically active neuropeptides called RF-amide neuropeptides. To explore more expansive sequence variation, preliminary studies were done by Ryan Maldonado using

1.0 mM of the RF-amide neuropeptide analogs.[11]All four RF-amide linear neuropeptide analogs tested by Ryan Maldonado induced structural transition of hPrP to amyloid like fibers.[11] The objective of the current study was to test the reproducibility of some of the peptides tested by Ryan Maldonado and to investigate the concentration dependence of RF-amide neuropeptides to induce amyloidosis. This study can report on any potential role of the amide cap in inducing structural transition of hPrP. It is also possible to elucidate any role of these naturally occurring RF-amide neuropeptides in the prion misfolding disorders.

The current work involved investigation of the following four synthetic neuropeptides: FMRF-amide (Phenylalanine-Methionine-Arginine-Phenylalanine), FLFQPQRF-amide (Phenylalanine-Leucine-Phenylalanine-Glutamine-Proline-Glutamine-Arginine-Phenylalanine), KGGFSFRF-amide (Lysine-Glycine-Glycine-Phenylalanine-Serine-Phenylalanine-Arginine-Phenylalanine) and VPNLPQRF-amide (Valine-Proline-Asparagine-Leucine-Proline-Glutamine-Arginine-Phenylalanine).

3.2 Results

3.2.1 Expression and purification of recombinant hPrP

Recombinant hPrP was expressed and purified from *E. coli* lysates following protocols as described in Chapter 2. Figure 3.1 shows the elution profile of the recombinant hPrP. Purified samples were run on SDS-PAGE to assess purity of hPrP. The SDS PAGE profile of the purified fractions is shown in Figure 3.2. The samples were judged to be ≥ 99% pure.

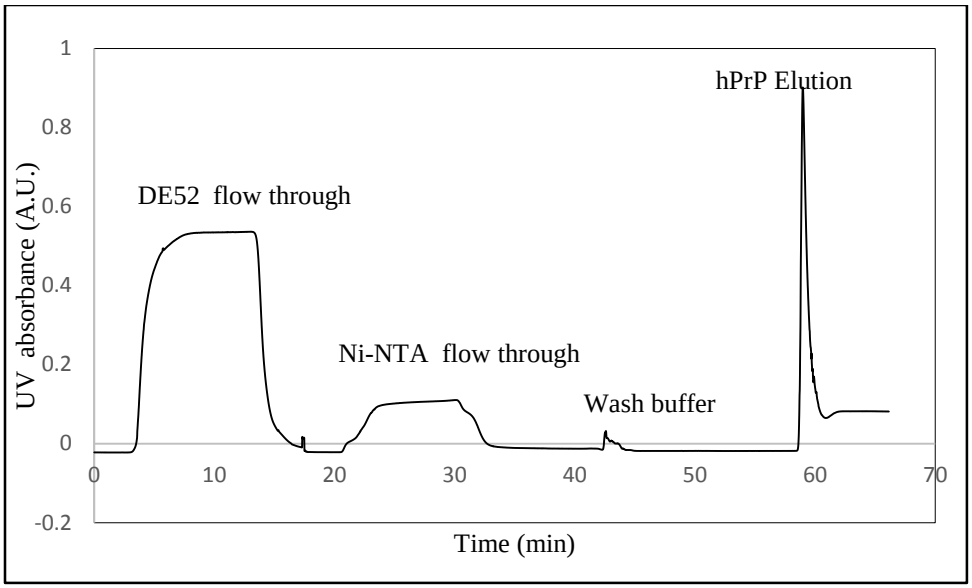

Figure 3.1 Elution profile of recombinant hPrP. The figure is a chromatogram for purification of recombinant hPrP using ion exchange and affinity. The cell lysate was loaded onto a DE52 column and the flow through was collected. The DE52 flow through was loaded onto Ni-NTA column. Prion protein has natural affinity to cationic nickel. Elution was achieved using 500 mM imidazole and by lowering the pH to 4.5 resulting in the large, sharp peak.

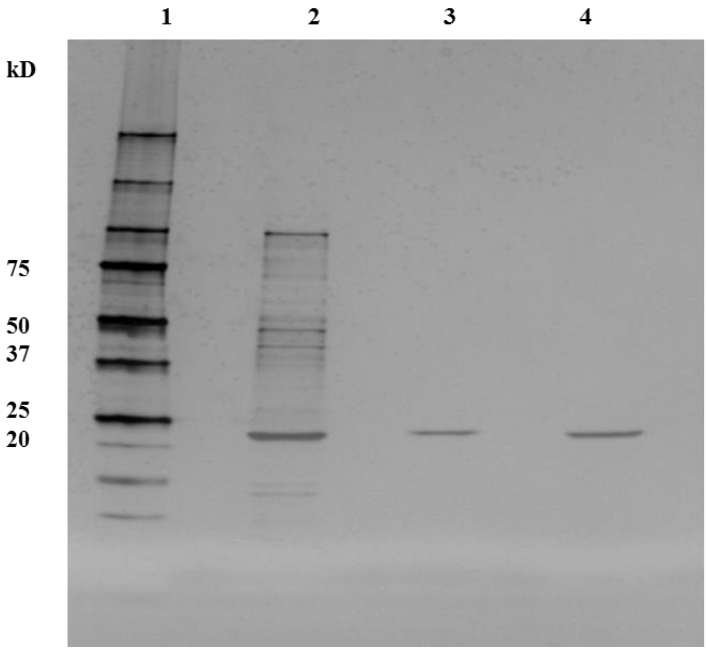

Figure 3.2 SDS-PAGE profile of purified fractions. The purified protein sample was analyzed by SDS-PAGE and silver stained as described in section 2.3.2. Lane 1 shows standard protein ladder. Lanes 2 shows the proteins in DE-52 flow through. Lane 3 shows Ni-NTA elution pre-dialysis and lane 4 shows Ni-NTA elution post-dialysis and filtration. Bands at ~23 kDa correspond to recombinant hPrP. Samples are judged to be ≥99% pure.

3.2.2 Native folding of recombinant hPrP

Native folding of the purified recombinant hPrP was determined by Circular Dichroism (CD) spectroscopy analysis. The native conformation of hPrP is predominantly α-helical structure. CD data as shown in Figure 3.3 showed the two local minima at ~210 and ~222 nm that are characteristics of the predominantly α-helical structures confirming the native folding of the purified recombinant hPrP.

In the study presented here, the amyloid conversion reactions were all performed at 37°C. Thermal denaturation of the purified hPrP was performed using CD spectroscopy to verify stability and native folding at the conversion reaction temperature of 37°C. Figure 3.4 shows the purified hPrP is stable and natively folded at 37°C.

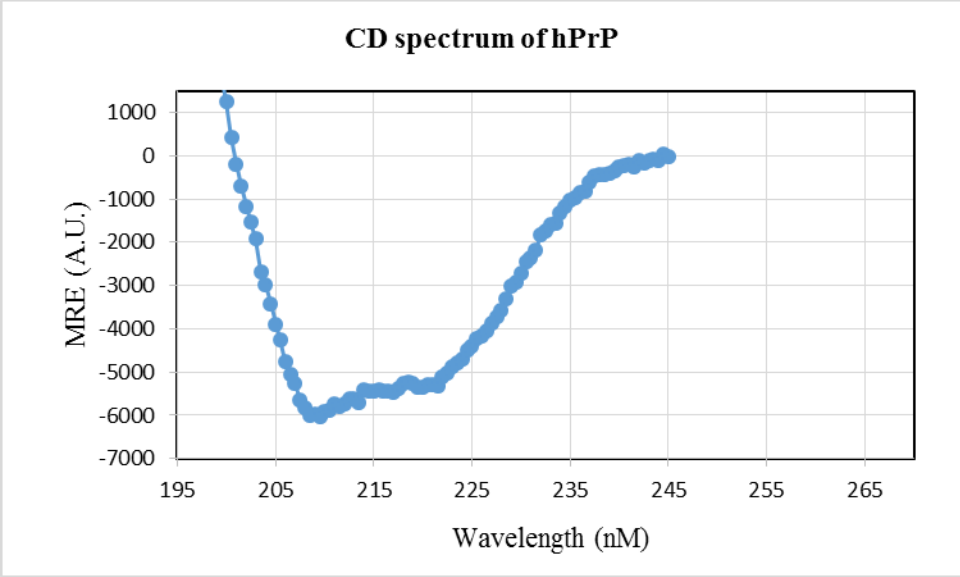

Figure 3.3 Circular dichroism spectrum of recombinant hPrP. The CD spectrum for hPrP was measured in 10 mM Na_2HPO_4 at room temperature. The concentration of hPrP in the sample was 0.2 mg/mL. The CD values are reported in units of deg $cm^2dmol^{-1}res^{-1}$. The two local minima in the spectrum at ~210 and ~222 nm indicate that hPrP was folded into predominantly α-helical structure.

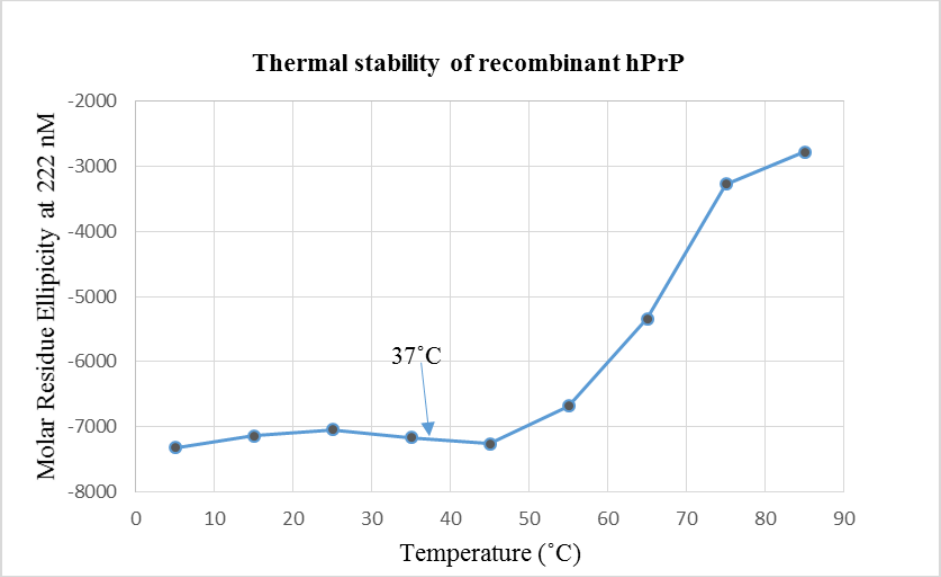

Figure 3.4 Thermal stability of recombinant hPrP. Thermal unfolding of recombinant hPrP was monitored by CD spectroscopy at 222 nm, which is indicative of α-helical content. This CD data indicates that hPrP is natively folded at 37°C, the temperature at which the peptide induced amyloid conversion reactions were performed.

3.2.3 RF-amide neuropeptide induced amyloidosis of hPrP

Prior work showed that synthetic peptides with KFAKF motifs can promote the conversion of natively folded hPrP to oligomers with amyloid-like properties. In the current study, we have tested the ability of synthetic RF-amide neuropeptides which have sequence similarity to KFAKF to induce amyloid formation of hPrP. As previously stated, the main focus of this study is to test the concentration dependence of the RF-amide neuropeptide analogs for converting native hPrP to amyloid-like fibrils. The following four synthetic neuropeptides were investigated: FMRF-amide (Phenylalanine-Methionine-Arginine-Phenylalanine), FLFQPQRF-amide (Phenylalanine-Leucine-Phenylalanine-Glutamine-Proline-Glutamine-Arginine-Phenylalanine), KGGFSFRF-amide (Lysine-Glycine-Glycine-Phenylalanine-Serine-Phenylalanine-Arginine-Phenylalanine) and VPNLPQRF-amide (Valine-Proline-Asparagine-Leucine-Proline-Glutamine-Arginine-Phenylalanine).

The concentration dependence of synthetic RF-amide neuropeptides for inducing amyloidosis was tested by the method described in Section 2.5. The method involved mixing 4.3 μM of hPrP with 1X PBS, 0.4% SDS, 0.4% Triton-X 100 and different concentrations (1.0 mM, 0.1 mM and 1.0 μM) of RF-amide neuropeptide analogs, followed by incubation at 37°C with agitation of 1500 RPM and intervals of 1 minute rest period for up to 72 hours. Amyloid conversion of natively folded hPrP was examined using SDD-AGE and PK digestion assay as described in Section 2.6. These assays are useful in determining if particles have distinct amyloid characteristics such as resistance to SDS denaturation and Proteinase K digestion.

Also, reactions were set up to determine if natively folded recombinant hPrP molecules would form amyloid fibrils under conversion reaction conditions in the absence of peptide. Figure 3.5 shows that in the absence of peptide, natively folded hPrP does not form detergent resistant oligomers on an SDD-AGE gel. PK resistant fragments were also not observed by the PK digestion assay as shown in Figure 3.6. The data served as negative control for the conversion reactions. This indicates that recombinant hPrP does not form amyloid fibrils under the reaction conditions in the absence of the peptide.

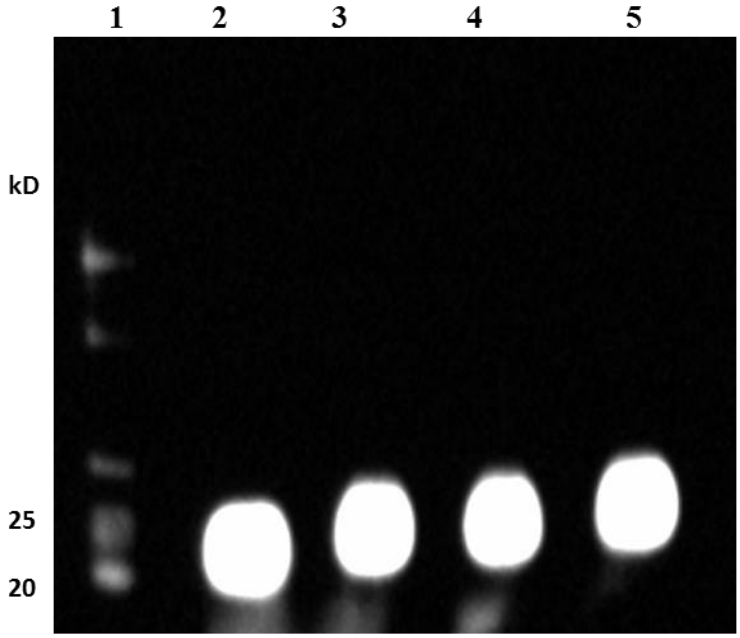

Figure 3.5 SDD-AGE analysis of hPrP in the absence of peptide. The SDD-AGE image shows conversion reaction of hPrP in the absence of peptide. Methods for the assay are as described above. Lane 1 is the protein ladder. Lane 2 contains monomeric hPrP. Lanes 3-5 contain samples of hPrP in the absence of peptide, allowed to react for 0, 48, 72 hours. Detergent resistant oligomers were not observed.

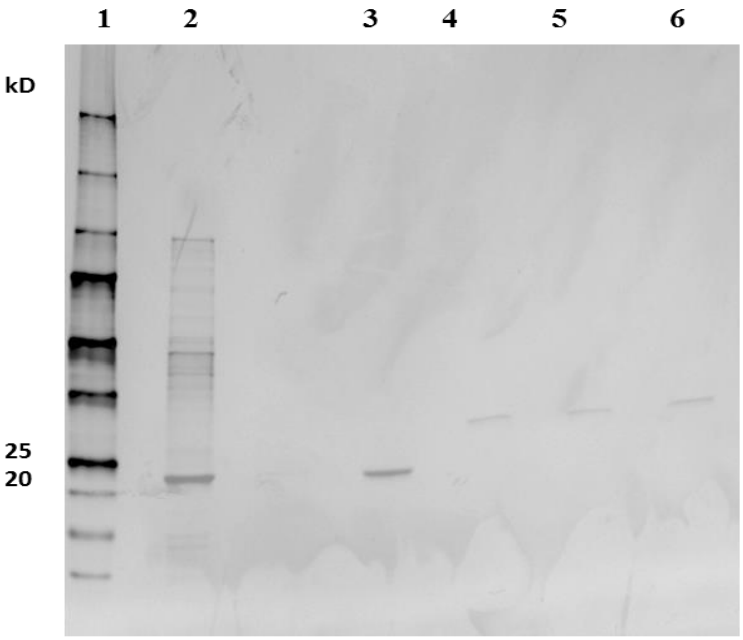

Figure 3.6 Proteinase K digestion of hPrP in the absence of peptide. The image shows results of PK digestion assay of hPrP in the absence of peptide. Lane 1 is the protein ladder. Lane 2 contains DE-52 flow through. Lane 3 contains monomeric hPrP which was not subjected to PK digestion. Lanes 4-6 contains samples of hPrP quenched at 0, 48, 72 hours which were subjected to PK digestion. The formation of a protease resistant core was not observed.

Concentration effects of the synthetic neuropeptide FMRF-amide to induce amyloidosis were tested by reacting hPrP with 1.0 mM, 0.1 mM and 1.0 µM of the peptide. SDD-AGE analysis was performed to test the ability of FMRF-amide to convert monomeric hPrP to SDS-resistant oligomers. Figure 3.7, Figure 3.9 and Figure 3.11 show that large detergent resistant oligomers were formed at all three concentrations at time points 24-72 hours. SDD-AGE images also show formation of a defined intermediate in all reactions from 24 hours onwards. As seen in Figure 3.8, Figure 3.10 and Figure 3.12, proteinase K digestion analyzed by SDS-PAGE also showed the formation of PK resistant fragments at all three concentrations 1.0 mM, 0.1mM and 1.0 µM of the peptide. These results indicate that the synthetic neuropeptide FMRF-amide can promote amyloid formation of recombinant hPrP at time point as early as 24 hours. The conversion of native hPrP into amyloid particles was not dependent on the concentration of FMRF-amide peptide in the range of the time points tested in this study.

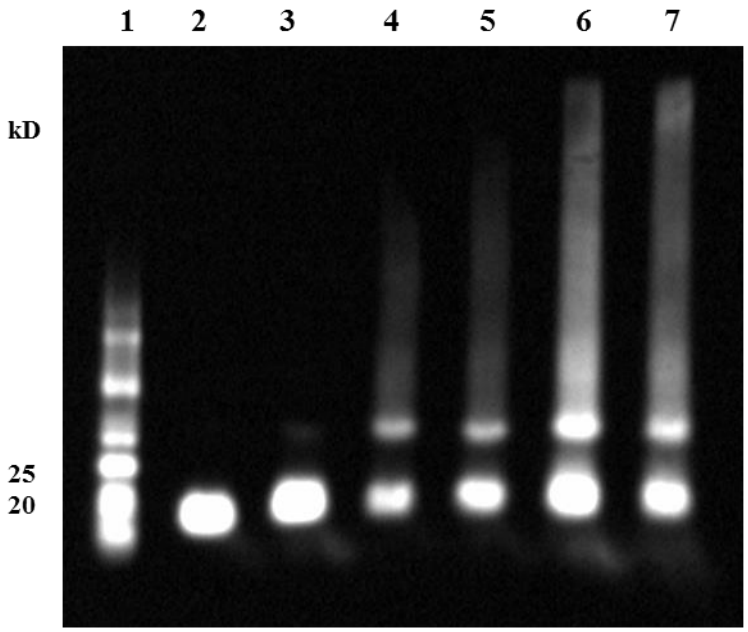

Figure 3.7 SDD-AGE of hPrP in the presence of 1.0 mM FMRF-amide neuropeptide analog. The image shows SDD-AGE of hPrP in the presence of 1.0 mM FMRF-amide. Lane 1 is the protein ladder. Lane 2 is the monomeric hPrP. Lanes 3-7 contain samples of hPrP mixed with 1.0 mM FMRF-amide peptide and incubated for 0, 24, 36, 48, and 72 hours. Lanes 4-7 show the formation of detergent resistant oligomers.

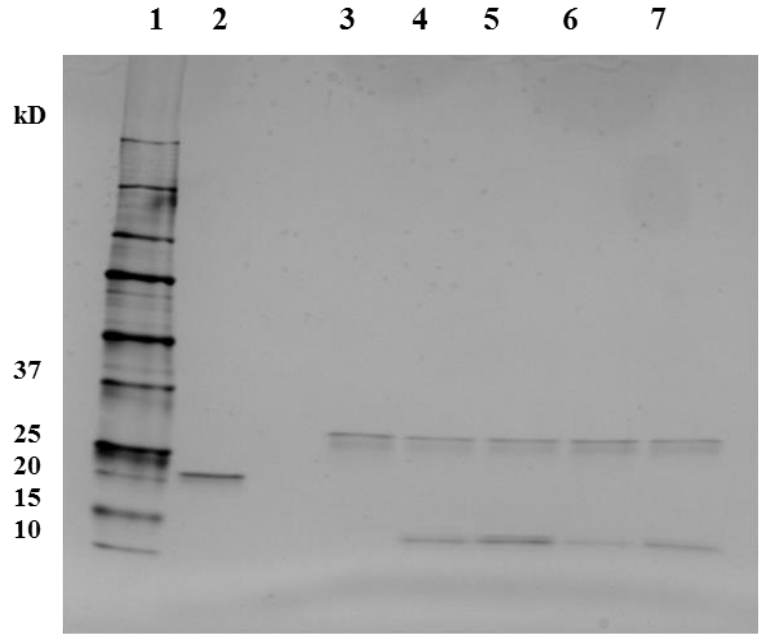

Figure 3.8 Proteinase K digestion of recombinant hPrP in the presence of 1.0 mM FMRF-amide neuropeptide analog. The image shows PK digestion of hPrP in the presence of 1.0 mM FMRF-amide. Lane 1 is the protein ladder. Lane 2 contains undigested monomeric hPrP. Lanes 3-7 contain samples of hPrP mixed with 1.0 mM FMRF-amide peptide and incubated for 0, 24, 36, 48, and 72 hours. Bands at 29 kDa correspond to PK. Lanes 4-7 show the formation of PK resistant core with sizes of around 14 kDa.

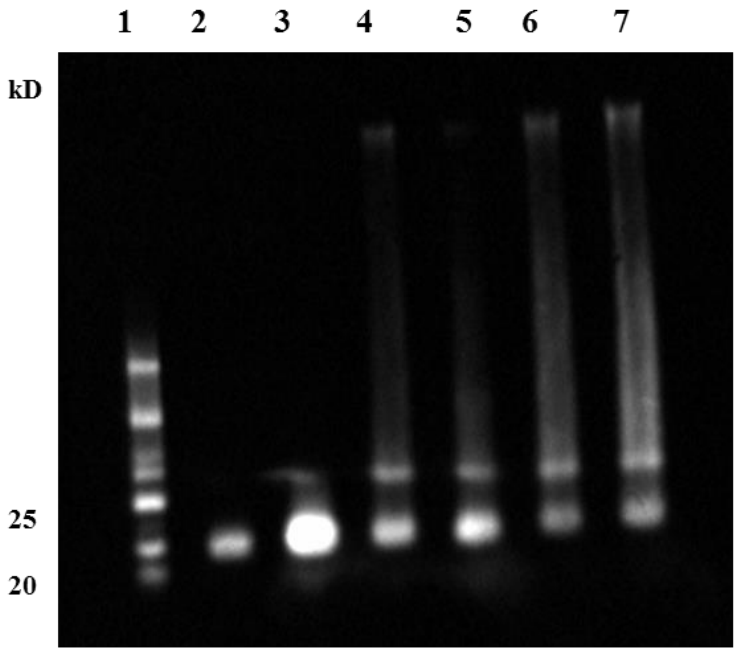

Figure 3.9 Conversion of monomeric hPrP to SDD-resistant oligomers by 0.1 mM FMRF-amide neuropeptide analog. The image shows SDD-AGE of hPrP in the presence of 0.1 mM FMRF-amide. Lane 1 is the protein ladder. Lane 2 is the monomeric hPrP. Lanes 3-7 contain samples of hPrP mixed with 0.1 mM FMRF-amide peptide and incubated for 0, 24, 36, 48, and 72 hours. Detergent resistant oligomers are observed from 24 hour time point onwards.

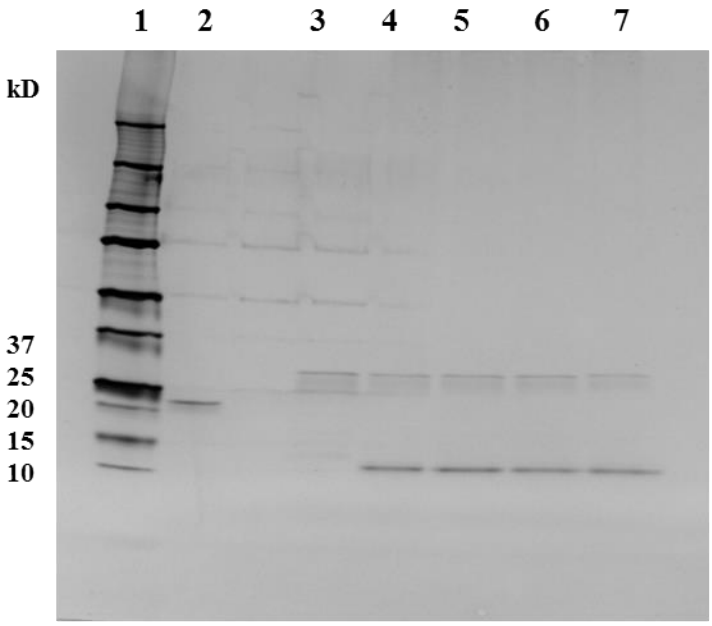

Figure 3.10 Proteinase K digestion of recombinant hPrP in the presence of 0.1 mM FMRF-amide neuropeptide analog. The image shows PK digestion of hPrP in the presence of 0.1 mM FMRF-amide. Lane 1 is the protein ladder. Lane 2 contains undigested monomeric hPrP. Lanes 3-7 contain samples of hPrP mixed with 0.1 mM FMRF-amide peptide and incubated for 0, 24, 36, 48, and 72 hours. Bands at 29 kDa correspond to PK. Lanes 4-7 show the formation of PK resistant core with sizes of around 12 kDa.

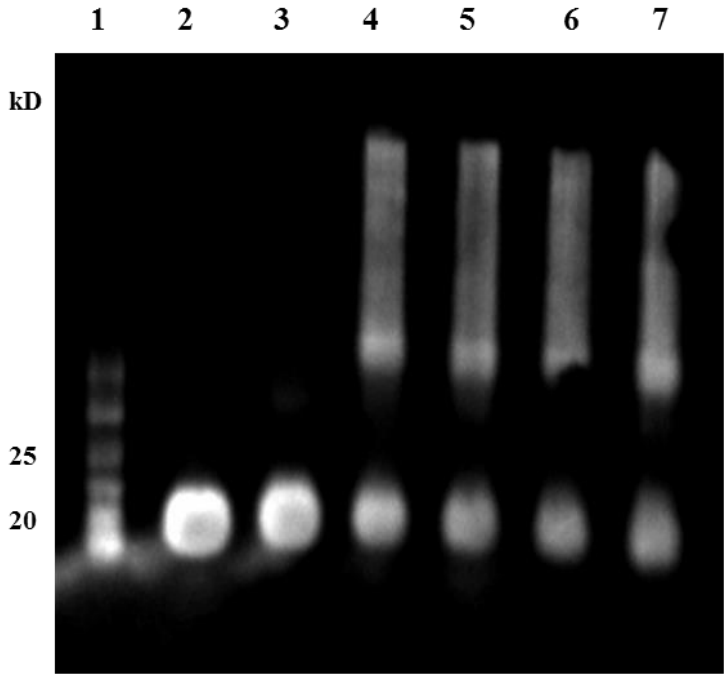

Figure 3.11 SDD-AGE analysis of hPrP in the presence of 1.0 µM FMRF-amide neuropeptide analog. The image shows SDD-AGE of hPrP in the presence of 1.0 µM FMRF-amide. Lane 1 is the protein ladder. Lane 2 is the monomeric hPrP. Lanes 3-7 contain samples of hPrP mixed with 1.0 µM FMRF-amide peptide and incubated for 0, 24, 36, 48, and 72 hours. Lanes 4-7 show formation of detergent resistant oligomers.

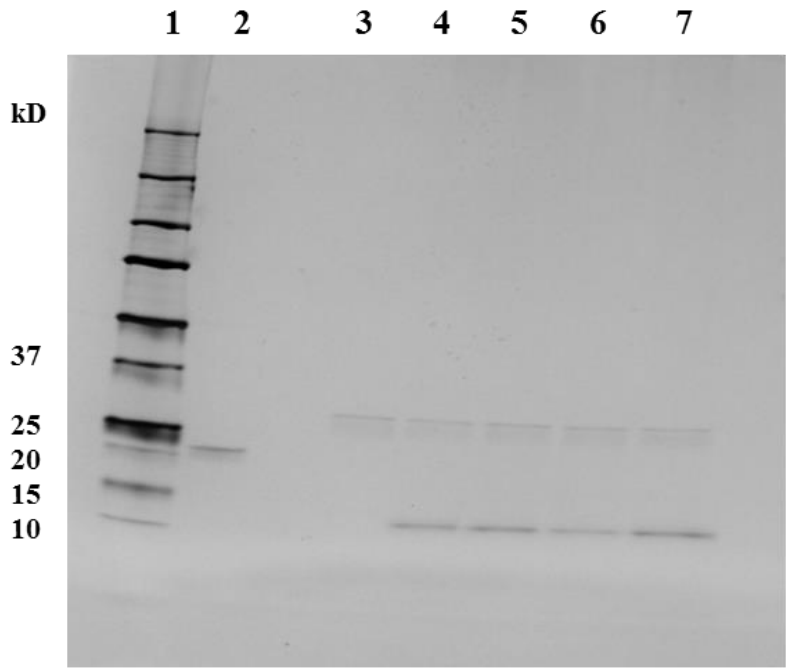

Figure 3.12 Proteinase K digestion of recombinant hPrP in the presence of 1.0 µM FMRF-amide neuropeptide analog. The image shows PK digestion of hPrP in the presence of 1.0 µM FMRF-amide. Lane 1 is the protein ladder. Lane 2 contains undigested monomeric hPrP. Lanes 3-7 contain samples of hPrP mixed with 1.0 µM FMRF-amide peptide and incubated for 0, 24, 36, 48, and 72 hours. Bands at 29 kDa correspond to PK. Lanes 4-7 show the formation of PK resistant fragments with sizes of around 12 kDa.

Recombinant hPrP incubated with synthetic neuropeptide FLFQPQRF-amide produced amyloid fibrils at 1.0 mM concentration. These reactions were performed as previously described for up to 72 hours with reactions quenched by freezing at different time points. Figure 3.13 shows SDD-AGE analysis of these reactions. Results show detergent resistant oligomers were formed after 36 hours. PK digestion assay results as seen on Figure 3.14 show formation of PK resistant fragments starting at 36 hours. These PK resistant fragments are much smaller than the undigested monomeric hPrP shown in lane 2. Unlike 1.0 mM conversion reactions, 0.1 mM FLFQPQRF-amide reactions did not show amyloid fibril formation. Figure 3.15 shows absence of any detergent resistant oligomers on SDD-AGE analysis. Also, as seen on Figure 3.16, PK digestion assay did not show any resistant fragments. These results indicate that a high concentration of 1.0 mM FLFQPQRF-amide peptide is required to induce amyloidosis of native hPrP. Reduction in peptide concentration by ten-fold does not induce amyloidosis of hPrP.

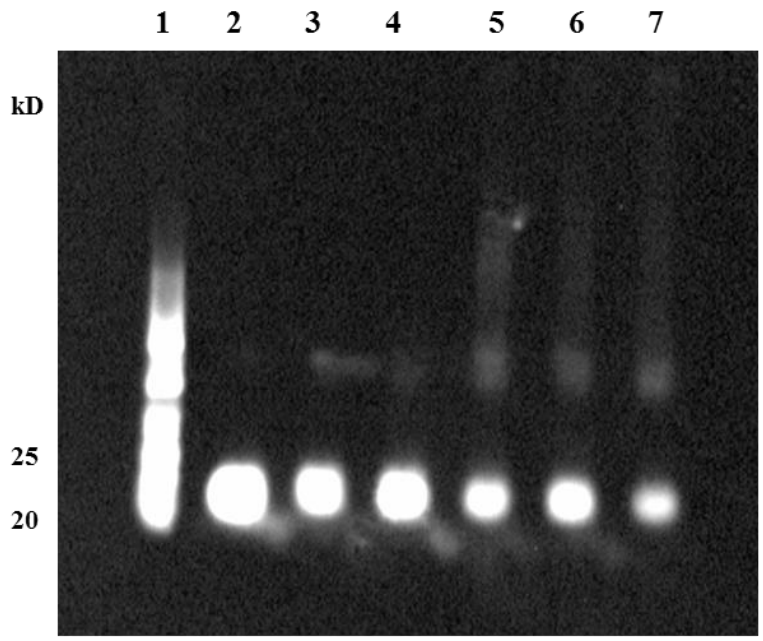

Figure 3.13 SDD-AGE of hPrP in the presence of 1.0 mM FLFQPQRF-amide neuropeptide analog. The image shows SDD-AGE of hPrP in the presence of 1.0 mM FLFQPQRF-amide. Lane 1 is the protein ladder. Lane 2 is the monomeric hPrP. Lanes 3-7 contain samples of hPrP mixed with 1.0 mM FLFQPQRF-amide peptide and incubated for 0, 24, 36, 48, and 72 hours. Lanes 5-7 show formation of detergent resistant oligomers.

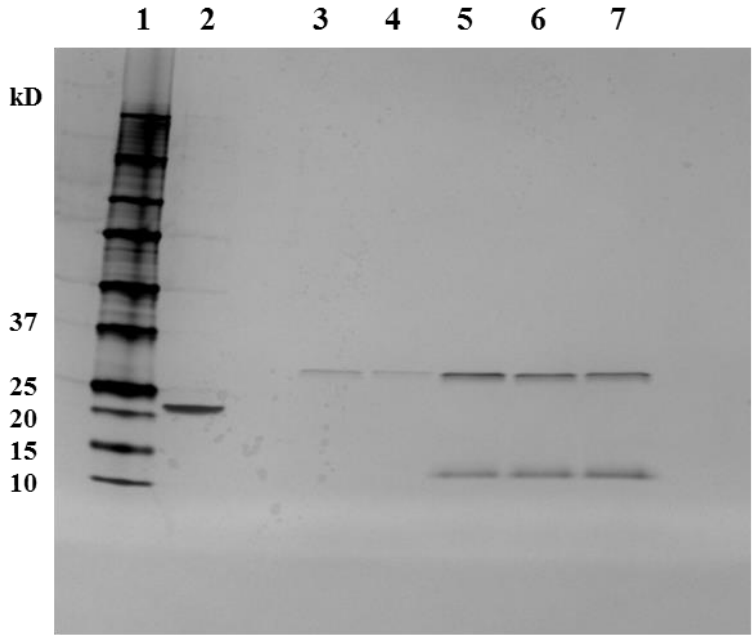

Figure 3.14 Proteinase K digestion of recombinant hPrP in the presence of 1.0 mM FLFQPQRF-amide neuropeptide analog. The image shows PK digestion of hPrP in the presence of 1.0 mM FLFQPQRF-amide. Lane 1 is the protein ladder. Lane 2 contains undigested monomeric hPrP. Lanes 3-7 contain samples of hPrP mixed with 1.0 mM FLFQPQRF-amide peptide and incubated for 0, 24, 36, 48, and 72 hours. Bands at 29 kDa correspond to PK. Lanes 5-7 show the formation of PK resistant fragments with sizes of around 12 kDa.

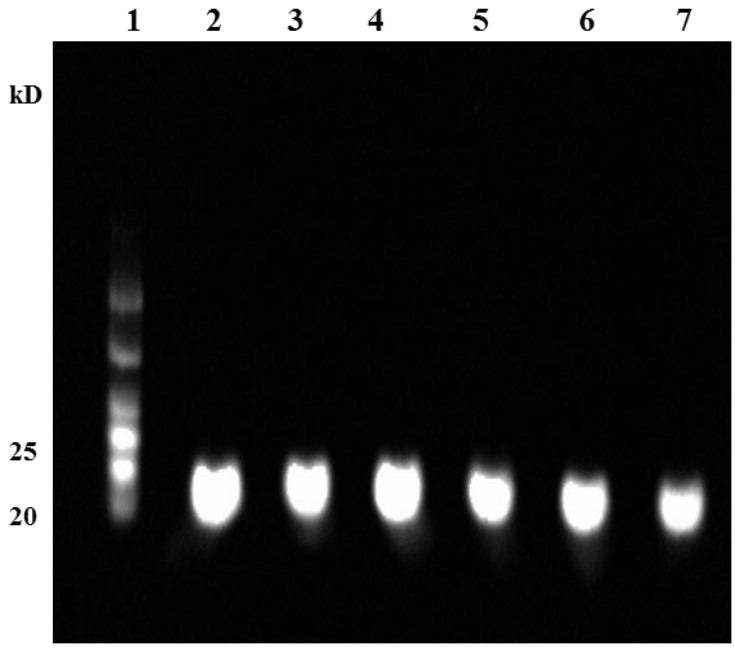

Figure 3.15 SDD-AGE of hPrP in the presence of 0.1 mM FLFQPQRF-amide neuropeptide analog. The image shows SDD-AGE of hPrP in the presence of 0.1 mM FLFQPQRF-amide. Lane 1 is the protein ladder. Lane 2 is the monomeric hPrP. Lanes 3-7 contain samples of hPrP mixed with 0.1 mM FLFQPQRF-amide peptide and incubated for 0, 24, 36, 48, and 72 hours. The formation of detergent resistant oligomers were not observed on these conversion reactions.

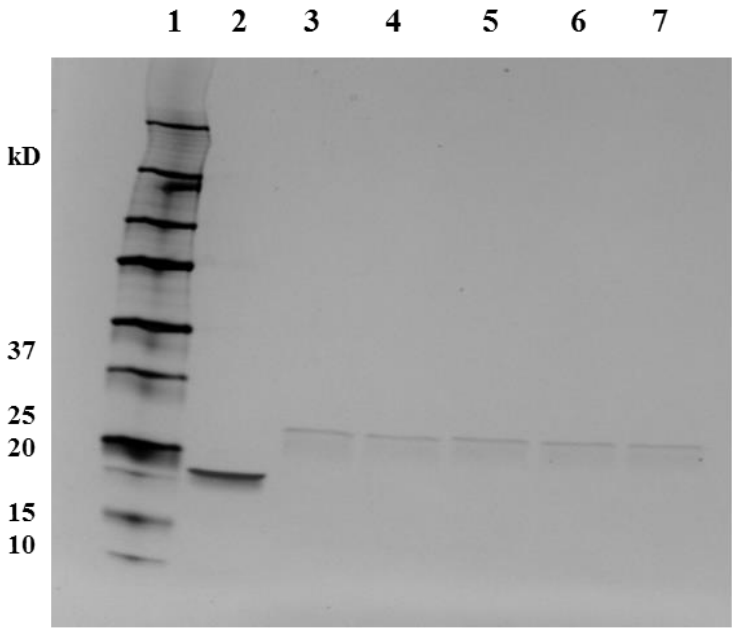

Figure 3.16 Proteinase K digestion of recombinant hPrP in the presence of 0.1 mM FLFQPQRF-amide neuropeptide analog. The image shows PK digestion of hPrP in the presence of 0.1 mM FLFQPQRF-amide. Lane 1 is the protein ladder. Lane 2 contains undigested monomeric hPrP. Lanes 3-7 contain samples of hPrP mixed with 0.1 mM FLFQPQRF-amide peptide and incubated for 0, 24, 36, 48, and 72 hours. Bands at 29 kDa correspond to PK. PK resistant fragments were not observed on these conversion reactions.

The synthetic neuropeptide KGGFSFRF-amide at 1.0 mM concentration after mixing with recombinant hPrP showed formation of oligomers with amyloid-like characteristics on SDD-AGE analysis. Figure 3.17 shows that SDS-resistant amyloid oligomers were detected from 12 hours onwards. This indicates that the KGGFSFRF-amide peptide reacts with hPrP in a short period of time to induce conformation change in the protein to form amyloid fibers. PK digestion assay results as shown in Figure 3.18 demonstrate resistant fragments from 12 hours. Concentration effects of the peptide was tested by reacting hPrP with 0.1 mM and 1.0 µM of KGGFSFRF-amide. Figure 3.19 shows SDD-AGE results of conversion reactions with 0.1 mM of the peptide. Large detergent resistant amyloid oligomers were observed from 24 hours' time point onwards. Proteinase K resistance was also observed after 24 hours as shown on Figure 3.20. Conversion reactions with 1.0 µM of KGGFSFRF-amide showed detergent resistant oligomers from 36 hours onwards, as shown on Figure 3.21. Figure 3.22 shows that PK resistant fragments were also observed at 36 hours' time point. These results indicate that the conversion of native hPrP into amyloid particles was dependent on the concentration of the peptide KGGFSFRF-amide in the reaction.

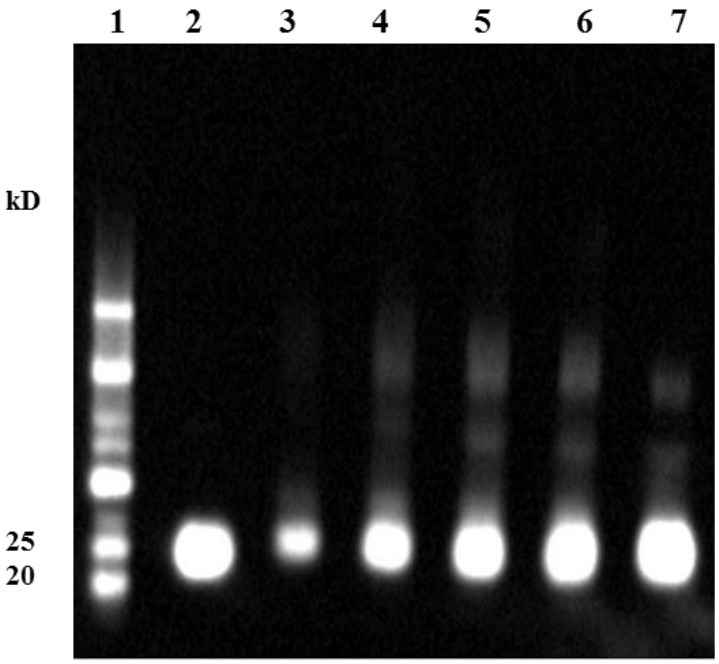

Figure 3.17 SDD-AGE of hPrP in the presence of 1.0 mM KGGFSFRF-amide neuropeptide analog. The image shows SDD-AGE of hPrP in the presence of 1.0 mM KGGFSFRF-amide. Lane 1 is the protein ladder. Lane 2 is the monomeric hPrP. Lanes 3-7 contain samples of hPrP mixed with 1.0 mM KGGFSFRF-amide peptide and incubated for 0, 12, 24, 48, and 72 hours. The formation of detergent resistant oligomers were observed on lanes 4-7.

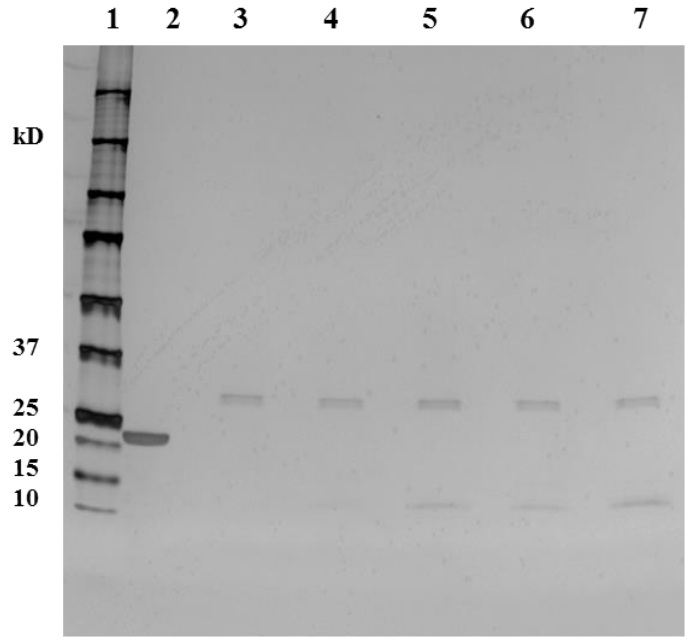

Figure 3.18 Proteinase K digestion of recombinant hPrP in the presence of 1.0 mM KGGFSFRF-amide neuropeptide analog. The image shows PK digestion of hPrP in the presence of 1.0 mM KGGFSFRF-amide. Lane 1 is the protein ladder. Lane 2 contains undigested monomeric hPrP. Lanes 3-7 contain samples of hPrP mixed with 1.0 mM KGGFSFRF-amide peptide and incubated for 0, 12, 24, 48, and 72 hours. Bands at 29 kDa correspond to PK. Lanes 4-7 show PK resistant fragments with sizes around 12 KDa.

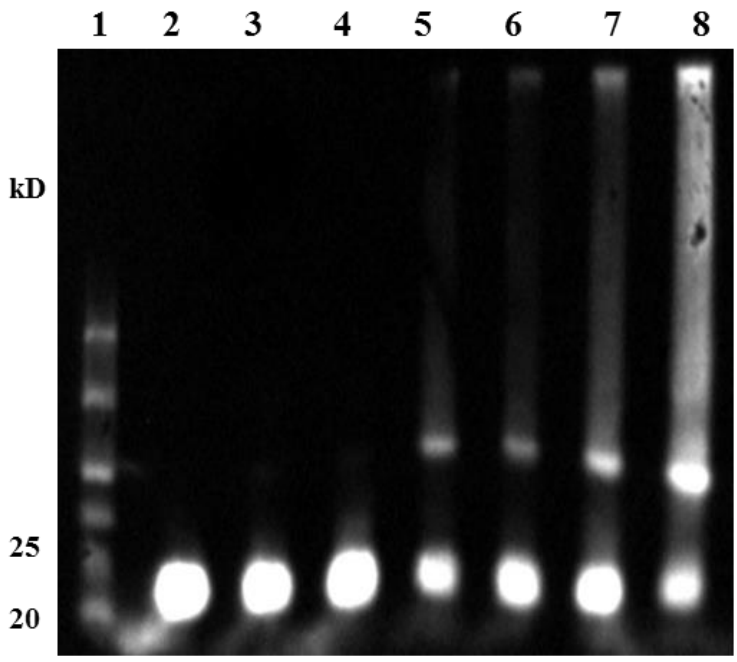

Figure 3.19 SDD-AGE of hPrP in the presence of 0.1 mM KGGFSFRF-amide neuropeptide analog. The image shows SDD-AGE of hPrP in the presence of 0.1 mM KGGFSFRF-amide. Lane 1 is the protein ladder. Lane 2 is the monomeric hPrP. Lanes 3-8 contain samples of hPrP mixed with 0.1 mM KGGFSFRF-amide peptide and incubated for 0, 12, 24, 36, 48, and 72 hours. Lanes 5-8 show formation of detergent resistant oligomers.

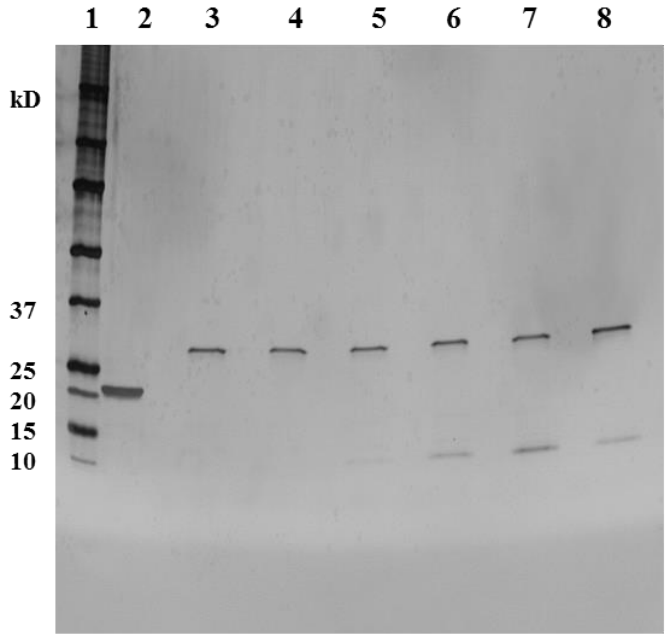

Figure 3.20 Proteinase K digestion of recombinant hPrP in the presence of 0.1 mM KGGFSFRF-amide neuropeptide analog. The image shows PK digestion of hPrP in the presence of 0.1 mM KGGFSFRF-amide. Lane 1 is the protein ladder. Lane 2 contains undigested monomeric hPrP. Lanes 3-8 contain samples of hPrP mixed with 0.1 mM KGGFSFRF-amide peptide and incubated for 0, 12, 24, 36, 48, and 72 hours. Bands at 29 kDa correspond to PK. Lanes 5-8 show PK resistant fragments with sizes around 12 KDa.

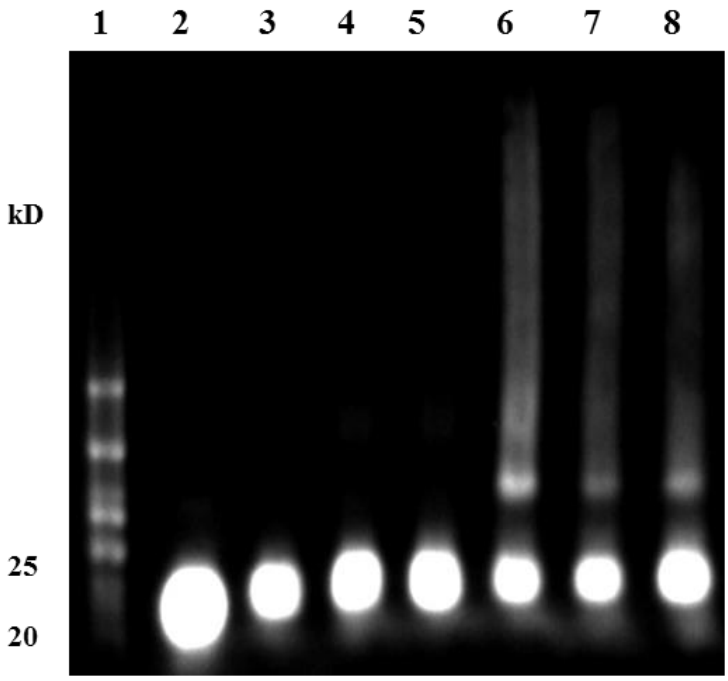

Figure 3.21 SDD-AGE of hPrP in the presence of 1.0 µM KGGFSFRF-amide neuropeptide analog. The image shows SDD-AGE of hPrP in the presence of 1.0 µM KGGFSFRF-amide. Lane 1 is the protein ladder. Lane 2 is the monomeric hPrP. Lanes 3-8 contain samples of hPrP mixed with 1.0 µM KGGFSFRF-amide peptide and incubated for 0, 12, 24, 36, 48, and 72 hours. Lanes 6-8 show formation of detergent resistant oligomers.

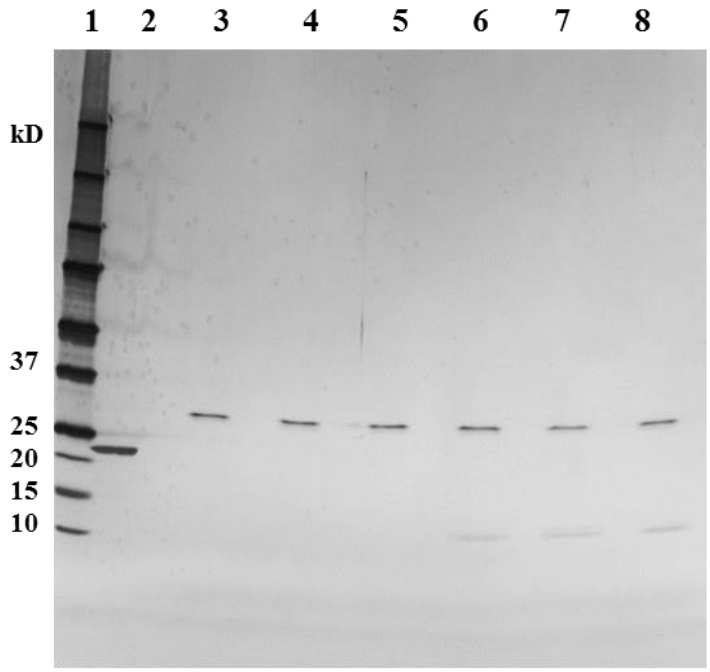

Figure 3.22 Proteinase K digestion of recombinant hPrP in the presence of 1.0 µM KGGFSFRF-amide neuropeptide analog. The image shows PK digestion of hPrP in the presence of 1.0 µM KGGFSFRF-amide. Lane 1 is the protein ladder. Lane 2 contains undigested monomeric hPrP. Lanes 3-8 contain samples of hPrP mixed with 1.0 µM KGGFSFRF-amide peptide and incubated for 0, 12, 24, 36, 48, and 72 hours. Bands at 29 kDa correspond to PK. Lanes 6-8 show PK resistant fragments with sizes around 12 KD.

Interestingly, the conversion reactions with 1.0 mM of the peptide VPNLPQRF-amide did not induce amyloidosis when reacted with hPrP. As seen in Figure 3.23, detergent resistant oligomers were not observed on SDD-AGE analysis. Also, all conversion reactions were completely digested by Proteinase K and no resistance was observed, as seen in Figure 3.24. These results indicate that even at a high concentration of 1.0 mM, the peptide VPNLPQRF-amide does not interact favorably with the binding site to induce amyloid formation.

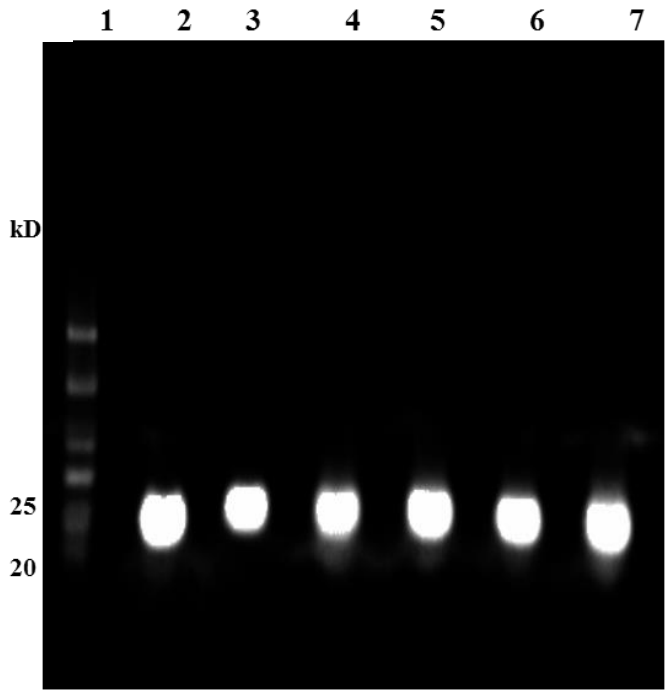

Figure 3.23 SDD-AGE of hPrP in the presence of 1.0 mM VPNLPQRF-amide neuropeptide analog. The image shows SDD-AGE of hPrP in the presence of 1.0 mM VPNLPQRF-amide. Lane 1 is the protein ladder. Lane 2 is the monomeric hPrP. Lanes 3-7 contain samples of hPrP mixed with 1.0 mM VPNLPQRF-amide peptide and incubated for 0, 24, 36, 48, and 72 hours. The formation of detergent resistant oligomers were not observed on these conversion reactions.

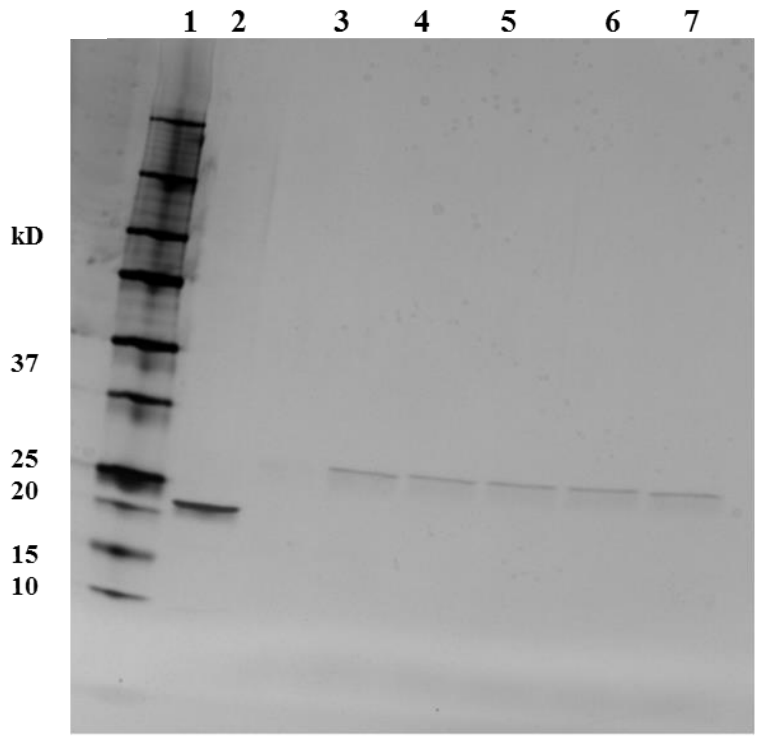

Figure 3.24 Proteinase K digestion of recombinant hPrP in the presence of 1.0 mM VPNLPQRF-amide neuropeptide analog. The image shows PK digestion of hPrP in the presence of 1.0 mM VPNLPQRF-amide. Lane 1 is the protein ladder. Lane 2 contains undigested monomeric hPrP. Lanes 3-7 contain samples of hPrP mixed with 1.0 mM VPNLPQRF-amide peptide and incubated for 0, 24, 36, 48, and 72 hours. Bands at 29 kDa correspond to PK. PK resistant fragments were not observed on these conversion reaction.

3.3 Discussion

The main objective of the current study was to establish concentration dependence of four synthetic RF-amide neuropeptides for converting native hPrP to amyloid-like fibrils. All four peptides tested in this study showed varying response in their ability to induce amyloidosis of hPrP. The rate of amyloid conversion appears to be sensitive to the sequence of the RF-amide neuropeptide. Changing the peptide sequence affects the interaction of the amino acid residues with the binding site of the protein, which could be the reason for varying concentration effects observed with the four peptides in their ability to induce amyloidosis.

SDD-AGE and PK digestion assay results showed that FMRF-amide peptide displayed highest efficacy in inducing amyloidosis of hPrP. Interestingly, previous studies showed that the sequence homolog RFMRF linear peptide did not induce amyloid formation of hPrP.[10] Probably, removal of the amino acid arginine from the N-terminal and addition of an amide cap in the C-terminal of the peptide favored binding with the predicted regulatory site of hPrP. The hydrophobic and charged-based favorable interactions of the FMRF-amide peptide with the regulatory site might have destabilized the native state of hPrP and induced a conformational change to an amyloid assembly competent state. Probably, concentration as low as 1.0 μM of the FMRF peptide was sufficient to overcome the energetic barrier between the native state and the amyloid competent state of hPrP. Therefore, decreasing the peptide concentration did not delay the duration of amyloid formation in the tested time points. The peptide KGGFSFRF-amide showed significant concentration dependence in its ability to induce amyloidosis of hPrP. SDD-AGE and PK digestion results show that decreasing the peptide

concentration from 1.0 mM to 1.0 µM increased the time required for amyloid fiber formation. This indicates that amyloidosis of hPrP was sensitive to the concentration of KGGFSFRF-amide peptide. The conversion reactions of hPrP with the peptide FLFQPQRF-amide showed amyloid formation only at 1.0 mM concentration. A high concentration of FLFQPQRF-amide peptide was needed to destabilize the native state and induce conformation change to amyloid assembly competent state. Conversion reactions with the peptide VPNLPQRF-amide did not show amyloid formation even at a high concentration of 1.0 mM. This indicates that the peptide sequence did not have favorable interactions with the regulatory site of hPrP to induce a global structural transition to amyloids. However, we cannot rule out the possibility that the peptide VPNLPQRF-amide is probably stabilizing the native functional state of hPrP. Further studies need to be done to probe their potential role in stabilizing the native state of hPrP.

The role of amide cap in inducing amyloidosis remains unclear. If the amide cap on the peptides was the sole factor in conversion, all four amidated peptides should have induced conversion of hPrP. However, only three of the four RF-amide peptides induced amyloidosis at a high concentration of 1.0 mM. This raises doubts on the possible role of the amide cap in amyloid conversion. Testing these peptide sequences without the amide cap and the linear peptide RFMRF with the amide cap can elucidate if the amide cap has any role in conversion. Further studies can be conducted to study the effect of the cyclic version of these amidated peptides in amyloid conversion reactions. These results would report on the potential for the RF-amide class of neuropeptides to contribute to prion disorders.

To understand ligand binding interactions, we can induce mutations at the predicted regulatory site of hPrP. NMR-based analysis of hPrP-peptide binding interactions can provide key molecular details for understanding structural transition of hPrP to amyloids. Additionally, studies could be conducted to test the ability of the peptides to block amyloid conversion of natively folded hPrP. This can potentially lead to the development of anti-prion peptidomimetics as drugs for treating prion disorders.

REFERENCES

(1) Hilser, V. J.; García-Moreno E, B.; Oas, T. G.; Kapp, G.; Whitten, S. T. A statistical thermodynamic model of the protein ensemble. *Chem. Rev.* **2006**, *106* (5), 1545–1558.

(2) Yang, L.-Q.; Sang, P.; Tao, Y.; Fu, Y.-X.; Zhang, K.-Q.; Xie, Y.-H.; Liu, S.-Q. Protein dynamics and motions in relation to their functions: several case studies and the underlying mechanisms. *J. Biomol. Struct. Dyn.* **2014**, *32* (3), 372–393.

(3) Hilser, V. J.; Freire, E. Structure-based calculation of the equilibrium folding pathway of proteins. Correlation with hydrogen exchange protection factors. *J. Mol. Biol.* **1996**, *262* (5), 756–772.

(4) Whitten, S. T.; García-Moreno E, B.; Hilser, V. J. Local conformational fluctuations can modulate the coupling between proton binding and global structural transitions in proteins. *Proc. Natl. Acad. Sci. U.S.A.* **2005**, *102* (12), 4282–4287.

(5) Liu, T.; Whitten, S. T.; Hilser, V. J. Functional residues serve a dominant role in mediating the cooperativity of the protein ensemble. *Proc. Natl. Acad. Sci. U.S.A.* **2007**, *104* (11), 4347–4352.

(6) Zahn, R.; Liu, A.; Lührs, T.; Riek, R.; von Schroetter, C.; López García, F.; Billeter, M.; Calzolai, L.; Wider, G.; Wüthrich, K. NMR solution structure of the human prion protein. *Proc. Natl. Acad. Sci. U.S.A.* **2000**, *97* (1), 145–150.

(7) Knaus, K. J.; Morillas, M.; Swietnicki, W.; Malone, M.; Surewicz, W. K.; Yee, V. C. Crystal structure of the human prion protein reveals a mechanism for oligomerization. *Nat. Struct. Biol.* **2001**, *8* (9), 770–774.

(8) Prusiner, S. B. Novel proteinaceous infectious particles cause scrapie. *Science* **1982**, *216* (4542), 136–144.

(9) Ma, J.; Wang, F. Prion disease and the "protein-only hypothesis." *Essays Biochem.* **2014**, *56*, 181–191.

(10) Adam, M. C. Peptide Induced Amyloidosis of Recombinant Human Prion Protein. *Thesis* **2012**.

(11) Maldonado, R. Testing the ability of RF-amide neuropeptides to promote amyloidosis of recombinant human prion protein. *Thesis* **2014**.

(12) Campbell, J. Optimization of SDD-AGE as a Method to Study Amyloid Conversion of Human Recombinant Prion Protein. *Thesis* **2014**.

(13) Qaiser, F.; Wahab, F.; Wiqar, M. A.; Hashim, R.; Leprince, J.; Vaudry, H.; Tena-Sempere, M.; Shahab, M. Study of the role of novel RF-amide neuropeptides in affecting growth hormone secretion in a representative non-human primate (Macaca mulatta). *Endocrine* **2012**, *42* (3), 658–663.

(14) Morales, R.; Callegari, K.; Soto, C. Prion-like features of misfolded Aβ and tau aggregates. *Virus Res.* **2015**, *207*, 106–112.

(15) Valastyan, J. S.; Lindquist, S. Mechanisms of protein-folding diseases at a glance. *Dis Model Mech* **2014**, *7* (1), 9–14.

(16) Ganchev, D. N.; Cobb, N. J.; Surewicz, K.; Surewicz, W. K. Nanomechanical properties of human prion protein amyloid as probed by force spectroscopy. *Biophys. J.* **2008**, *95* (6), 2909–2915.

(17) Puckett, C.; Concannon, P.; Casey, C.; Hood, L. Genomic structure of the human prion protein gene. *Am. J. Hum. Genet.* **1991**, *49* (2), 320–329.

(18) Chen, W.; van der Kamp, M. W.; Daggett, V. Structural and dynamic properties of the human prion protein. *Biophys. J.* **2014**, *106* (5), 1152–1163.

(19) Zomosa-Signoret, V.; Arnaud, J.-D.; Fontes, P.; Alvarez-Martinez, M.-T.; Liautard, J.-P. Physiological role of the cellular prion protein. *Vet. Res.* **2008**, *39* (4), 9.

(20) Aguilar-Calvo, P.; García, C.; Espinosa, J. C.; Andreoletti, O.; Torres, J. M. Prion and prion-like diseases in animals. *Virus Res.* **2015**, *207*, 82–93.

(21) Yau, J.; Sharpe, S. Structures of amyloid fibrils formed by the prion protein derived peptides PrP(244-249) and PrP(245-250). *J. Struct. Biol.* **2012**, *180* (2), 290–302.

(22) Maji, S. K.; Wang, L.; Greenwald, J.; Riek, R. Structure-activity relationship of amyloid fibrils. *FEBS Lett.* **2009**, *583* (16), 2610–2617.

(23) Langkilde, A. E.; Vestergaard, B. Methods for structural characterization of prefibrillar intermediates and amyloid fibrils. *FEBS Lett.* **2009**, *583* (16), 2600–2609.

(24) Halfmann, R.; Lindquist, S. Screening for amyloid aggregation by Semi-Denaturing Detergent-Agarose Gel Electrophoresis. *J Vis Exp* **2008**, No. 17.

(25) Concha-Marambio, L.; Diaz-Espinoza, R.; Soto, C. The extent of protease resistance of misfolded prion protein is highly dependent on the salt concentration. *J. Biol. Chem.* **2014**, *289* (5), 3073–3079.

(26) Whitmore, L.; Wallace, B. A. Protein secondary structure analyses from circular dichroism spectroscopy: methods and reference databases. *Biopolymers* **2008**, *89* (5), 392–400.

(27) Ebeling, W.; Hennrich, N.; Klockow, M.; Metz, H.; Orth, H. D.; Lang, H. Proteinase K from Tritirachium album Limber. *Eur. J. Biochem.* **1974**, *47* (1), 91–97.

(28) Ostapchenko, V. G.; Sawaya, M. R.; Makarava, N.; Savtchenko, R.; Nilsson, K. P. R.; Eisenberg, D.; Baskakov, I. V. Two amyloid States of the prion protein display significantly different folding patterns. *J. Mol. Biol.* **2010**, *400* (4), 908–921.